



LAWRENCE  
LIVERMORE  
NATIONAL  
LABORATORY

UCRL-JRNL-213064

# Galactic Bulge Microlensing Events from the MACHO Collaboration

C. L. Thomas, K. Griest , P. Popowski, K. H. Cook, A. J. Drake, D. Minniti, D. G. Myer, C. Alcock, R. A. Allsman, D. R. Alves, T. S. Axelrod, A. C. Becker, D. P. Bennett, K. C. Freeman, M. Geha, M. J. Lehner, S. L. Marshall, C. A. Nelson, B. A. Peterson, P. J. Quinn, C. W. Stubbs, W. Sutherland, T. Vandehei, D. L. Welch

June 20, 2005

Astrophysical Journal

## **Disclaimer**

---

This document was prepared as an account of work sponsored by an agency of the United States Government. Neither the United States Government nor the University of California nor any of their employees, makes any warranty, express or implied, or assumes any legal liability or responsibility for the accuracy, completeness, or usefulness of any information, apparatus, product, or process disclosed, or represents that its use would not infringe privately owned rights. Reference herein to any specific commercial product, process, or service by trade name, trademark, manufacturer, or otherwise, does not necessarily constitute or imply its endorsement, recommendation, or favoring by the United States Government or the University of California. The views and opinions of authors expressed herein do not necessarily state or reflect those of the United States Government or the University of California, and shall not be used for advertising or product endorsement purposes.

## **Galactic Bulge Microlensing Events from the MACHO Collaboration**

C.L. Thomas<sup>1</sup>, K. Griest<sup>1</sup>, P. Popowski<sup>2</sup>, K.H. Cook<sup>3</sup>, A.J. Drake<sup>4</sup>, D. Minniti<sup>4</sup>, D.G. Myer<sup>1</sup>,  
C. Alcock<sup>5</sup>, R.A. Allsman<sup>6</sup>, D.R. Alves<sup>7</sup>, T.S. Axelrod<sup>8</sup>, A.C. Becker<sup>9</sup>, D.P. Bennett<sup>10</sup>,  
K.C. Freeman<sup>11</sup>, M. Geha<sup>12</sup>, M.J. Lehner<sup>13</sup>, S.L. Marshall<sup>14</sup>, C.A. Nelson<sup>3</sup>, B.A. Peterson<sup>11</sup>,  
P.J. Quinn<sup>15</sup>, C.W. Stubbs<sup>5</sup>, W. Sutherland<sup>16</sup>, T. Vandehei<sup>1</sup>, D.L. Welch<sup>17</sup>

(The MACHO Collaboration)

## Abstract

---

<sup>1</sup>Department of Physics, University of California, San Diego, CA 92093, USA  
Email: `clt`, `kgriest`, `dmyer@ucsd.edu`, `vandehei@astrophys.ucsd.edu`

<sup>2</sup>Max-Planck-Institute for Astrophysics, Karl-Schwarzschild-Str. 1, Postfach 1317, 85741 Garching bei München, Germany  
Email: `popowski@mpa-garching.mpg.de`

<sup>3</sup>Lawrence Livermore National Laboratory, Livermore, CA 94550, USA  
Email: `kcook`, `cnelson@igpp.ucllnl.org`

<sup>4</sup>Departamento de Astronomia, Pontifica Universidad Catolica, Casilla 104, Santiago 22, Chile  
Email: `dante`, `ajd@astro.puc.cl`

<sup>5</sup>Harvard-Smithsonian Center for Astrophysics, 60 Garden St., Cambridge, MA 02138, USA  
Email: `calcock`, `cstubbs@cfa.harvard.edu`

<sup>6</sup>NOAO, 950 North Cherry Ave., Tucson, AZ 85719, USA  
Email: `robyn@noao.edu`

<sup>7</sup>Laboratory for Astronommy & Solar Physics, Goddard Space Flight Center, Code 689, Greenbelt, MD 20781, USA  
Email: `alves@astro.columbia.edu`

<sup>8</sup>Steward Observatory, University of Arizona, Tucson, AZ 85721, USA  
Email: `taxelrod@as.arizona.edu`

<sup>9</sup>Astronomy Department, University of Washington, Seattle, WA 98195, USA  
Email: `becker@astro.washington.edu`

<sup>10</sup>Department of Physics, University of Notre Dame, IN 46556, USA  
Email: `bennett@emu.phys.nd.edu`

<sup>11</sup>Research School of Astronomy and Astrophysics, Canberra, Weston Creek, ACT 2611, Australia  
Email: `kcf`, `pетerson@mso.anu.edu.au`

<sup>12</sup>Carnegie Observatories, 813 Santa Barbara Street, Pasadena, CA 91101, USA  
Email: `mgeha@ociw.edu`

<sup>13</sup>Department of Physics and Astronomy, University of Pennsylvania, PA 19104, USA  
Email: `mlehner@hep.upenn.edu`

<sup>14</sup>SLAC/KIPAC, 2575 Sand Hill Rd., MS 29, Menlo Park, CA 94025, USA  
Email: `marshall@slac.stanford.edu`

<sup>15</sup>European Southern Observatory, Karl-Schwarzchild-Str. 2, 85748 Garching bei München, Germany  
Email: `pjq@eso.org`

<sup>16</sup>Institute of Astronomy, University of Cambridge, Madingley Road, Cambridge. CB3 0HA, U.K.  
Email: `wjs@ast.cam.ac.uk`

<sup>17</sup>McMaster University, Hamilton, Ontario Canada L8S 4M1  
Email: `welch@physics.mcmaster.ca`

We present a catalog of 450 relatively high signal-to-noise microlensing events observed by the MACHO collaboration between 1993 and 1999. The events are distributed throughout our fields and, as expected, they show clear concentration toward the Galactic center. No optical depth is given for this sample since no blending efficiency calculation has been performed, and we find evidence for substantial blending. In a companion paper we give optical depths for the sub-sample of events on clump giant source stars, where blending is a less significant effect.

Several events with sources that may belong to the Sagittarius dwarf galaxy are identified. For these events even relatively low dispersion spectra could suffice to classify these events as either consistent with Sagittarius membership or as non-Sagittarius sources. Several unusual events, such as microlensing of periodic variable source stars, binary lens events, and an event showing extended source effects are identified. We also identify a number of contaminating background events as cataclysmic variable stars.

*Subject headings:* catalogs, gravitational lensing, Galaxy: bulge, Galaxy: structure, stars: dwarf novae, stars: variables: other

## 1. Introduction

The structure and composition of our Galaxy is one of the outstanding problems in contemporary astrophysics. While inventories of bright stars have been made, it is known that the bulk of the material in our Galaxy is dark. In addition, the number and mass distribution of stellar remnants such as white dwarfs, neutron stars and black holes is quite uncertain, as is the number of faint stars, brown dwarfs and extra-solar planets. Gravitational microlensing was suggested as a probe to detect compact objects including dark matter (Paczynski 1986, Griest 1991a, Nemiroff 1991) and was observationally discovered in 1993 (Alcock et al. 1993; Aubourg et al. 1993; Udalski et al. 1993). The line-of-sight towards the Large Magellanic Cloud (LMC) is best for dark matter detection, but as a probe of faint objects from planets to black holes, the line-of-sight towards the Galactic bulge is superior (Griest et al. 1991b; Paczynski 1991). The high density of stars in the disk and bulge means that the vast majority of events detected by microlensing experiments are in this direction.

The amount of lensing matter between a source and the observer is typically described using the optical depth to microlensing,  $\tau$ , defined as the probability that a given source star will be magnified by any lens by more than a factor of 1.34. Early predictions (Griest et al. 1991b; Paczynski 1991) of the optical depth towards the Galactic center included only disk lenses and found values

near  $\tau = 0.5 \times 10^{-6}$ . The early detection rate (Udalski et al. 1993, 1994a) seemed higher than this, and further calculations (Kiraga & Paczyński 1994) added bulge stars to bring the prediction up to  $0.85 \times 10^{-6}$ . The first measurements were substantially higher than this,  $\tau \geq 3.3 \pm 1.2 \times 10^{-6}$  (Udalski et al. 1994b) based upon 9 events and  $\tau = 3.9_{-1.2}^{+1.8}$  (Alcock et al. 1997) based upon an efficiency calculation and 13 clump-giant events taken from their 45 candidates. Many additional calculations ensued, including additional effects, especially non-axisymmetric components such as a bar (e.g. Zhao, Spergel & Rich 1995; Metcalf 1995; Zhao & Mao 1996; Bissantz et al. 1997; Gyuk 1999; Nair & Miralda-Escudé 1999; Binney, Bissantz & Gerhard 2000; Sevenster & Kalnajs 2001; Evans & Belokurov 2002; Han & Gould 2003). Values in the range  $0.8 \times 10^{-6}$  to  $2 \times 10^{-6}$  were predicted for various models, and values as large  $\tau = 4 \times 10^{-6}$  were found to be inconsistent with almost any model.

More recent measurements have all used efficiency calculations and have found values of  $\tau = 2.43_{-0.38}^{+0.39} \times 10^{-6}$  from 99 events in 8 fields using difference imaging (Alcock et al. 2000b; MACHO),  $\tau = 2.59_{-0.64}^{+0.84}$  from 28 events using difference imaging analysis (Sumi et al. 2003; MOA)<sup>1</sup>,  $\tau = 2.0 \pm 0.4 \times 10^{-6}$  from around 50 clump-giant events in a preliminary version of the companion paper (Popowski et al. 2001a; MACHO), and  $\tau = 0.94 \pm 0.29 \times 10^{-6}$  from 16 clump-giant events (Afonso et al. 2003; EROS).

In releases similar in spirit to our catalog here Udalski et al. (2000) presented a catalog of 214 microlensing events from the 3 seasons of the OGLE-II bulge observation, and Woźniak et al. (2001) presented a catalog of 520 events.

In this work we present our complete catalog of high signal-to-noise microlensing events that were found with point spread function fitting photometry. In the companion paper (Popowski et al. 2004), we make an accurate determination of the bulge optical depth using the 62 clump giant events (60 unique) listed here and find  $\tau = 2.17_{-0.38}^{+0.47} \times 10^{-6}$  at  $(l, b) = (1^\circ 50, -2^\circ 68)$ . We do not calculate an optical depth for our entire sample of microlensing events since a complete blending efficiency calculation has not been performed, and we caution against using the entire sample of events for such purposes.

Initially envisioned as a probe of dark matter, microlensing has evolved into a more general astronomical tool, useful for several distinct purposes. For example, since the duration of the microlensing event is proportional to the square root of the lens mass, microlensing is sensitive to compact objects in the  $10^{-7} M_\odot$  to  $10^1 M_\odot$  range, independent of the object’s luminosity, so

---

<sup>1</sup>The optical depth values found with difference image analysis require an adjustment for disk-disk lensing, the details of which can be found in the referenced papers. This adjustment increases the optical depth toward the bulge by roughly 25%.

it facilitates inventories of brown dwarfs, white dwarfs, and black holes. However, the lens mass measurement is degenerate with the lens distance and speed, severely limiting the accuracy of the mass distribution measurement. Our catalog includes several long duration events that may be massive black holes and several short duration events that may be brown dwarfs.

In order to break the mass/distance/speed degeneracy several techniques have been applied to rare classes of events such as those with binary lenses, binary sources, large annual parallaxes, etc. Our catalog lists events which may be members of exotic microlensing classes. Finally microlensing has emerged as a powerful method of detecting or constraining the existence of extra-solar planets orbiting the lens (Mao & Paczyński 1991; Gould & Loeb 1992; Griest & Safizadeh 1998; Rie et al. 2000; Gaudi et al. 2002). A key for these searches is careful follow-up on microlensing events, almost all of which are towards the Galactic bulge. Our catalog can be used to determine the frequencies of detectable lensing in various directions towards the bulge.

For comparison with other works we note that our definition of microlensing event duration,  $\hat{t}$ , is the Einstein ring diameter crossing time, twice the more commonly used Einstein ring radius crossing time.

## 2. Data

The MACHO Project had full-time use of the 1.27 meter telescope at Mount Stromlo Observatory, Australia<sup>2</sup> from July 1992 until December 1999. Details of the telescope system are given by Hart et al. (1996), and details of the camera system by Stubbs et al. (1993) and Marshall et al. (1994). Briefly, corrective optics and a dichroic were used to give simultaneous imaging of a  $43' \times 43'$  field in two non-standard filter bands, using eight  $2048 \times 2048$  pixel CCD's. A total of 32700 exposures were taken in 94 fields towards the Milky Way bulge, resulting in around 3 Tbytes of raw image data and photometry on 50.2 million stars. The location of the centers of the bulge fields are shown in Figure 1 and the location and number of exposures taken of each field are given in Table 1. Table 1 also gives the number of stars in each field, the number of clump giants, the number of microlensing events, and the sampling efficiency at event durations of  $\hat{t} = 50$  and  $\hat{t} = 200$  days. This latter numbers can be used as a rough indication of the relative sensitivity to microlensing in each field, but should be used for quantitative work only with the clump giant sample of events (see the companion paper by Popowski et al. 2004). The coverage of fields varies greatly from 12 observations of field 106 to 1815 observations of field 119. Note that the observing strategy changed several times during the project, so even in a given field the frequency of observations changed

---

<sup>2</sup>A fire tragically razed Mount Stromlo Observatory in January of 2003.

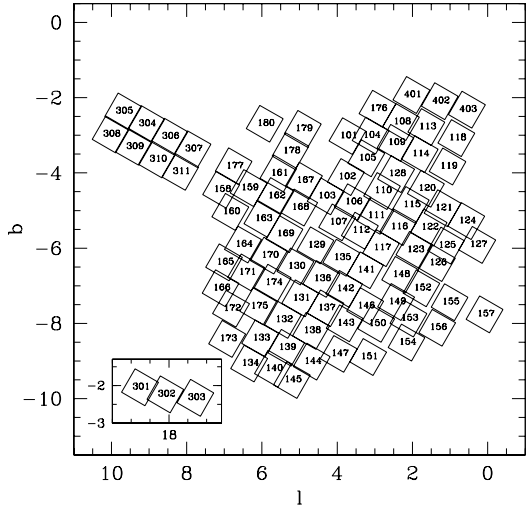


Fig. 1.— Location of the bulge fields in galactic coordinates

from year to year. In addition, there are gaps between November and February as the bulge was not observed during prime LMC observing times.

The photometric reduction used here is a variation of the DOPHOT (Schechter, Mateo, & Saha 1993) point spread function (PSF) fitting method (Alcock et al. 1999). Briefly, a good-quality image of each field is chosen as a template and used to generate a list of stellar positions and magnitudes. The templates are used to “warm-start” all subsequent photometric reductions, and for each star we record information on the flux, an error estimate, the object type, the  $\chi^2$  of the PSF fit, a crowding parameter, a local sky level, and the fraction of the star’s flux rejected due to bad pixels and cosmic rays. The resulting data are reorganized into lightcurves, and searched for variable stars and microlensing events. The photometric data base used here is about 450 Gbytes in size. We report magnitudes using global photometric relations that express Johnsons  $V$  and Kron-Cousins  $R$  in terms of the MACHO intrinsic magnitudes  $b_M$  and  $r_M$  as:

$$V = b_M - 0.18(b_M - r_M) + 23.70 \quad (1)$$

$$R = r_M + 0.18(b_M - r_M) + 23.41. \quad (2)$$

For more details see Alcock et al. (1999).

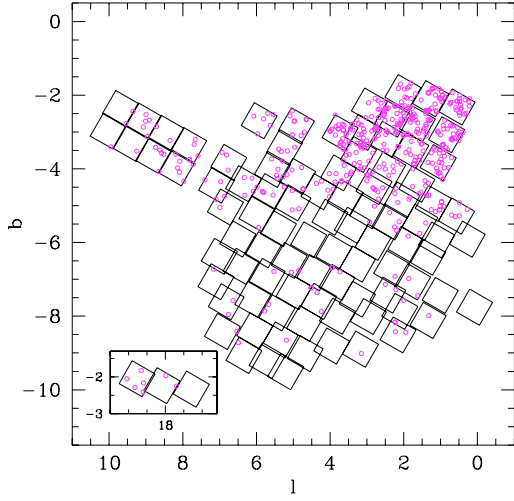


Fig. 2.— Spatial distribution of microlensing events. The scarcity of events with  $b = 6$  is due mainly to the small number of observations of fields in that region and thus very low detection efficiencies.

### 3. Event selection

The data set used here consists of about 19 billion individual photometric measurements. Discriminating genuine microlensing from stellar variability, systematic photometry errors, and other astronomical events is difficult, and the significance of the results depend upon the event selection criteria. The selection criteria are based on cuts made on a set of over 150 statistics calculated for each lightcurve. First a smaller set of “level 1” statistics is calculated for every star in the data base. Based on variability criteria, a few percent of the lightcurves are advanced to level 1 and the complete set of statistics, including non-linear fits to microlensing lightcurve shape, are calculated. Using these a broad selection of events is advanced to level 1.5 and output. Finally a fine-tuned set of selection criteria is used to select the level 2 candidates. From a total of 50.2 million lightcurves, around 90000 were advanced to level 1.5, and 337 to level 2. In addition, during this procedure, lightcurves are tagged as variable stars for inclusion in our variable star catalog.

If the goal is to measure the optical depth or microlensing rate, then great care must be taken in the selection of candidate microlensing events. It is crucial that the same selection method be performed on the actual data and on the artificial data used to calculate the detection efficiency. A certain fraction of “good” microlensing events will be missed by any set of selection criteria, and

it is important to not include these events in any calculation of optical depth. For more discussion, the reader is referred to the companion paper (Popowski et al. 2004) that derives the microlensing optical depth toward the Galactic bulge based on clump giant events.

The basic cuts of selection criteria “c”<sup>3</sup> are given in Table 2. A more thorough description of the most useful statistics is given in Alcock et al. (2000c). Note that Table 2 below is not intended to fully inform about the selection of bulge events; instead it is supposed to document the level 2 selection criteria used. Nevertheless in column 2 we offer a rough guide to what a given cut or class of cuts is intended to achieve.

In this paper, however, since no estimate of optical depth is being made, we can augment the computer selected (criteria “c”) events with “good” events found by other methods such as our alert system (Alcock et al. 1996) or even a search by eye over a larger set of candidates. In Figure 2 we show the position of the microlensing events on the sky. In Figure 10 we display the lightcurves of events we selected, organized by field.tile.seq identification number. In Tables 3 and 4 we describe the source stars corresponding to the selected events, and also give the microlensing fit parameters. Table 3 contains the events we subjectively regard as likely microlensing candidates, while Table 4 shows the events we think are probably not microlensing. Column 10 of Tables 3 and 4 shows our subjective “grade” of the event data quality (A-F). Column 11 shows the method or methods by which each event was selected (‘c’  $\mapsto$  “criteria c”, ‘a’  $\mapsto$  “alert system”, ‘b’  $\mapsto$  “binary search”, ‘e’  $\mapsto$  “by eye selection” out of an expanded set of events from a “c”-like selection). Column 12 shows our subjective determination of event type (‘CV’  $\mapsto$  suspected cataclysmic variable or supernova, ‘var’  $\mapsto$  suspected variable star, ‘bin’  $\mapsto$  suspected binary lensing event, ‘ $R \neq B$ ’  $\mapsto$  red and blue lightcurves differ in shape and/or amplitude indicating a possible blend or systematic error). In column 1 we also mark events identified as lensed clump giants in the companion paper with a † flag. We also include OGLE event identifications in Table 5 for events found at the same position in both surveys.

Note, that for the clump giant subsample used to calculate optical depth it is important that very few non-microlensing events are selected by the “c” criteria. However, when we apply the “c” criteria to non-clump areas of the color-magnitude diagram a few non-microlensing events are selected. This is not a problem for optical depth calculation but may be of interest. We list the entire set of events that pass criteria “c”, including 5 events which we subjectively graded as probably non-microlensing (quality D or F or suspected variable) in Table 4.

In summary we show the lightcurves of 252 grade “A” (very good signal-to-noise) candidate

---

<sup>3</sup>We use lowercase “c” to denote the computerized clump-like selection criteria, a capital “C” is used when referring to our subjective grades of events.

microlensing events, 198 grade “B” (good quality) events, and 76 grade “C” (poor quality) events. Of the grade “A” events 220 were selected with criteria “c”, 6 from the alert system, 4 from our binary search, and 22 by eye. Of the grade “B” events 97 were found with criteria “c”, 15 with the alert system, 2 from the binary search, and 84 by eye. Of the grade “C” events 11 were selected with criteria “c”, 12 by the alert system, 1 from our binary search, and 52 by eye. We also identify 32 pairs of candidates at the same location on the sky and one triplet of events. These are either the same physical events reported in two overlapping fields (14 cases) or two stars so close on the sky that they both receive the flux from the actual event (20 cases). This latter effect results from the photometry code and not the microlensing of two separate sources. In such cases we move the worse of the two events into Table 4, and recommend ignoring it.

#### 4. Special events

##### 4.1. Binaries

Alcock et al. (2000a) described 17 binaries in the Galactic bulge. We include these events in the lightcurve figures and in the tables. We also mark 24 additional events as potential binaries. These are events that have deviations from the standard lightcurve shape and may be better fit with a binary lens or source lightcurve. We have not done this fitting in this paper, and it is also possible that these are not microlensing or have larger than normal measurement errors.

##### 4.2. Lensing of variable stars

Several of the good quality microlensing events occurred on periodic, or nearly periodic variable stars. These include events: 108.18689.1979, 108.19602.415, 118.18009.35, and 403.47848.35.

These events are useful because the measured amplitude of the stellar variation allows one to determine the amount of blending. If the variability can be used to learn more about these stars (such as their distance or radius) then in some cases the degeneracy between lens mass, distance, and velocity may be partly broken.

##### 4.3. Other exotic events

Event 121.22423.1032 seems to display extended source effects.

## 5. Supernovae and Cataclysmic Variables

Supernova (SN) explosions in galaxies behind the microlensing source stars have been shown to contribute a significant background to the LMC and SMC microlensing searches (Alcock et al. 2000c). We do not expect SN to be as important in this search towards the Galactic bulge due to the large extinction through the disk and bulge, but we did a search for SN-like lightcurves, and have marked a number of events that we think are not microlensing. In fact, most of these events are probably cataclysmic variables (CV), e.g., novae or dwarf novae (DNe), so we mark them as ‘CV’. Of the 16 events we identify in this way, 7 repeat, i.e. show more than one brightening. Most of these events exhibit a rapid rise ( $\sim 4$  days) followed by a more gradual decline ( $\sim 20$  days). The peak is typically about 4 magnitudes brighter in  $V$  and 2.7 magnitudes brighter in  $R$  than the baseline, consistent with the CV classification (Sterken & Jaschek, 1996). We identify these events as CV’s rather than SNe because the decline after peak is too fast over the first 20 days as compared with typical SN.

The lightcurves of the repeating CV’s can be seen in Figure 10. We classify these as long period dwarf novae, since the periods seem to be between 300 and 700 days. In particular note: event 113.18676.5195 with 7 outbursts and a period of around 400 days, event 114.19842.2283 with 5 outbursts and a period of around 340 days, event 115.22695.3361 with 3 outbursts, as well events with two outbursts: 178.23266.2918, 178.24048.3166, and 311.37730.4143.

Since our photometry points are generally separated by at least one day, no flickering analysis is done. In dwarf novae one expects flickering on time scales of minutes to hours, so further observations are needed to positively identify these source as DNe. The 9 events with single excursions are more difficult to identify; possibilities include long duration DNe, or heavily blended classical novae. They are unlikely to be SNe.

## 6. The significance of blending

The photometry code measures the light coming from stars within the seeing disk, and for bulge stars and conditions at Mt. Stromlo Observatory this means there are usually many stars contained within each photometric “object”. However, in almost all cases only the light from one of these stars is lensed and gives rise to the transient microlensing lightcurve. The light from the non-lensed source therefore “blends” with the light from the lensed source distorting the lightcurve from its theoretical shape. In particular the event duration  $\hat{t}$  derived from a fit to a blended lightcurve can be shortened and the magnification decreased. Since the microlensing optical depth is proportional to the durations of the events, blending must be taken into account when trying to measure an

optical depth.

In the companion paper (Popowski et al. 2004), we show that when using clump giant stars as sources the problem of blending is alleviated. In the events on non-clump stars listed in this paper, however, blending is expected to be quite significant. One signature of a heavily blended event is a large difference between the magnification in the red and blue filter bands. In Tables 3 and 4 we label events which have such a large difference as “ $R \neq B$ ”. These differences may be due to blending, or especially for the lower quality events (grade C) these differences may just be indicating that the event is not microlensing.

## 7. Signatures of Sagittarius dwarf galaxy

Sagittarius dwarf galaxy (Ibata, Gilmore, & Irwin 1995) is the closest satellite galaxy to the Milky Way at a distance of about 25 kpc from the Sun. It is centered at the globular cluster M54 at  $(l, b) = (5^\circ.6, -14^\circ.0)$ , and extends over several degrees perpendicular to the Galactic plane. Traces of Sgr dwarf structure can be seen behind the MACHO fields that lie at negative Galactic latitudes. Therefore, we expect that some microlensing events may originate in Sgr dwarf. The identification of events with sources in the Sgr dwarf serves several goals: 1. it removes the contaminating sources from the map of the microlensing optical depth toward the Galactic bulge and thus improves the determination of bar parameters; 2. it probes the inner 25 kpc of the Galaxy for massive dark structures; 3. it helps to constrain the mass function of the lenses. We discuss these points in more detail below.

To fully explore the results of the microlensing surveys, we would like to better understand the lens population. In particular, we want to assign the lenses to different Galactic populations. However, because most of the lenses are too faint to be directly observed, we attempt to use the location of the sources to constrain the location of the lenses. We can assume that the sources in the Galactic bulge imply that the lenses are either in the bulge or in the disk and that the sources in the Sagittarius dwarf galaxy should typically have lenses in the bulge. By finding events that have Sgr sources, we can make better maps of the microlensing optical depth toward the sources in the bulge. Such improved maps will provide crucial constraints in constructing better models of the Galactic bar. It is even possible that a detailed analysis of events with Sgr sources could reveal a lens population *behind* the Galactic bulge. Such a population could be part of the warped or flared disk or even of a new, as yet undiscovered streamer of stars. In brief, Sgr events probe the inner 25 pc of the Galaxy for intervening structures in a way not possible with microlensing events with sources in the bulge.

A separate goal is to constrain the masses of the lenses. The distribution of the durations of

events contains the information about the masses of the lenses and the kinematics of the objects involved in the lensing process. However, a characteristic time of microlensing event is a degenerate combination of several parameters, including the geometry of the system and the relative transverse velocity. The better constraints we have on the kinematics, the better we can understand the masses of the lenses. For example, Gould (2000) showed that the bulge velocity dispersion introduces so much scatter to the duration distribution that lenses in the form of brown dwarfs cannot be distinguished from those in the form of neutron stars on an event-by-event basis. Therefore, the situations where kinematics is additionally constrained are very valuable. There are a few generic cases that help to determine the masses of the lenses: 1) the parallax effect, which places constraints on the combination of the relative velocity and distances (Bennett et al. 2002), 2) the measurement of the relative proper motion of the lens with respect to the source, which is particularly powerful if coupled with a parallax measurement (Alcock et al. 2001), 3) the possibility to assign a source to a system with distinct bulk velocity and negligible velocity dispersion (e.g., Sagittarius dwarf galaxy). We think the time is ripe to explore this third option. The large extent to which the identification of the microlensing events with sources in Sagittarius dwarf galaxy would improve the determination of the masses of the lenses can be judged from Fig. 8 by Cseresnjes & Alard (2001). Moreover, such events can probe a different lens population than all the other techniques used thus far. Cases 1) and 2) are biased toward detecting the lenses in the disk, whereas the lenses for Sgr events would likely be in the Galactic bulge or may even be behind the bulge.

Is it possible to select Sgr events based on their expected location on a color-magnitude diagram (CMD) from the MACHO survey? This is illustrated in Figure 3, where we show the sources of microlensing events detected by the MACHO collaboration on a  $V_0$  versus  $(V - R)_0$  CMD. The CMD was dereddened using the extinction map by Popowski, Cook, & Becker (2003) [extinction  $A_V$  was taken from column 4 of their Table 3]. In panel a) we plot the microlensing events together with a ridge-line (bold lines) of the Sgr dwarf galaxy taken from Bellazzini et al. (1999). The ridge-line has been adjusted to the dereddened quantities using  $E(V - I) = 0.22$  and  $A_V = 0.55$ . The ridge-line in  $(V - R)_0$  color has been derived assuming that  $(V - R)_0 = 0.5(V - I)_0$ , which according to Padova isochrones (Girardi et al. 2002: the tables provided on their web page: <http://pleiadi.pd.astro.it>) is accurate to within a few percent. The intrinsic width of the observed stellar distribution in Sgr dwarf is visualized with thin solid lines (only for the bluer branch of the Bellazzini et al. 1999 track). The errors of  $(V - R)_0$  color of the MACHO events are of order of at least 0.05 mag. We conclude that many microlensing events could have sources in Sgr dwarf galaxy. In panel b) we superpose relevant Padova isochrones on the same collection of events. The blue isochrone is for an age of 12.6 Gyr and metallicity [M/H] of  $-1.7$ , the green one for an age of 10.0 Gyr and metallicity  $-1.3$ , and the red one for an age of 6.3 Gyr and metallicity of  $-0.4$  (which is claimed to be the dominant population according to Monaco et al. 2002). We shifted

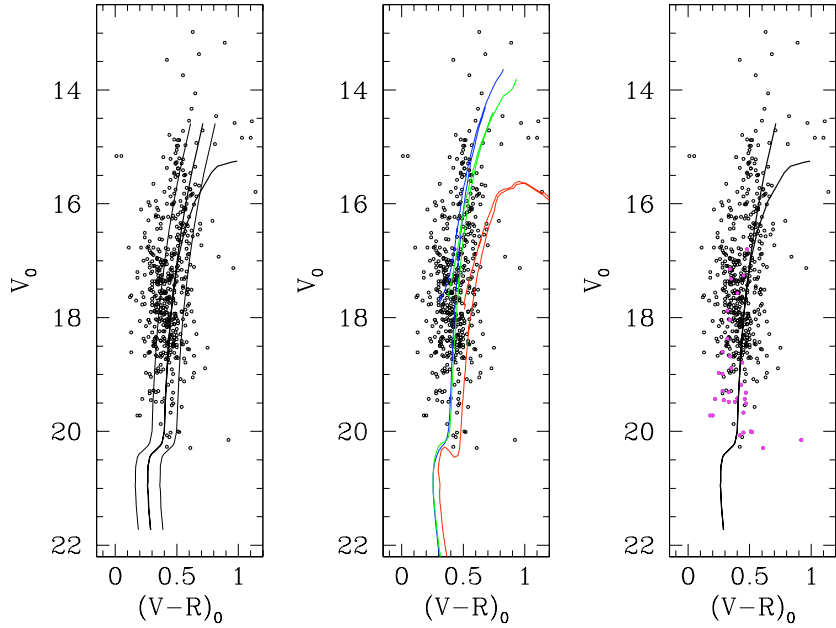


Fig. 3.— In panel a) we plot the events together with a ridge-line (bold lines) of the Sgr dwarf galaxy taken from Bellazzini et al. (1999). The intrinsic width of the observed stellar distribution in Sgr dwarf is visualized with thin solid lines (only for the bluer branch of the Bellazzini et al. 1999 track). The errors of  $(V - R)_0$  color of the MACHO events are of order of at least 0.05 magnitudes. In panel b) we superpose relevant Padova isochrones on the same collection of events. The solid isochrone (colored blue in the electronic edition) is for an age of 12.6 Gyr and metallicity [M/H] of  $-1.7$ , the long dashed one (solid green in the electronic edition) for an age of 10.0 Gyr and metallicity  $-1.3$ , and the short dashed one (solid red in the electronic edition) for an age of 6.3 Gyr and metallicity of  $-0.4$ . We shifted the isochrones assuming the distance modulus,  $(m - M)_{\text{Sgr}} = 17.0$ . From panels a) and b) we conclude that many microlensing events are consistent with having sources in the Sgr dwarf galaxy. Therefore, the location of events on the  $(V, V - R)$  color-magnitude diagram does not facilitate the identification of Sgr sources. In panel c), the events with the Galactic latitude  $b < -6.0$  are circled (marked as solid magenta dots in the electronic edition). Their distribution on a CMD is not identical to the other events and many of them are more consistent with Sgr membership. Again we over-plotted a ridge-line from Bellazzini et al. (1999) for reference.

the isochrones assuming the distance modulus,  $(m - M)_{\text{Sgr}} = 17.0$ . Again, many microlensing events are consistent with having sources in the Sgr dwarf galaxy. Therefore, the location of events on the  $(V, V - R)$  color-magnitude diagram does not facilitate the identification of Sgr sources.

Is there any way to narrow the list of possible Sgr events? Kunder, Popowski, & Cook (2005, in preparation) analyzed a set of almost 4000 RR Lyrae stars in the MACHO bulge fields. They separated the stars into the bulge and Sgr groups with high confidence. The Sgr RR Lyrae stars dominate over the bulge ones for Galactic latitudes  $b < -6.0$ . This suggests that Sgr sources can make a detectable contribution to the microlensing optical depth at these latitudes, which is in qualitative agreement with conclusions from Cseresnjes & Alard (2001). In panel c) of Figure 3, the microlensing events with the Galactic latitude  $b < -6.0$  are marked as solid magenta dots. Their distribution on a CMD is not identical to the other events, which is apparent from the distribution of their dereddened  $V_0$  magnitudes (Figure 4). In addition, many of those events are in the vicinity of the Sgr ridgeline suggesting that they are more consistent with Sgr membership. These 34 events are our Sgr dwarf candidates. We list their main parameters in Table 6. We warn, however, that the distinct character of events at  $b < -6.0$  may be at least partly unrelated to the presence of Sagittarius dwarf galaxy. To the zeroth order, our microlensing events are randomly drawn from the luminosity function at a given position of the sky. If the dereddened luminosity function for fields with  $b < -6.0$  peaks at a fainter magnitude than for the fields closer to the plane, the microlensing events in outer fields will tend to be fainter in the dereddened CMD.

The Sagittarius dwarf galaxy has a heliocentric radial velocity of  $140 \pm 10$  km/s, very different from the bulk of bulge stars (see e.g. Figure 4 by Ibata et al. 1995). The Sgr membership cannot be assigned in a robust way based on the measurement of radial velocities alone, but such measurements are very powerful in eliminating bulge or disk events. In addition, radial velocity can be obtained long after the event. Our 34 candidates are the recommended targets for such an investigation<sup>4</sup>.

Our selection of Sgr microlensing candidates should enable the first systematic search for such stars by the means of radial velocities. There are two recent spectroscopic studies of microlensing events toward the Galactic bulge by Cavallo et al. (2002) and Kane & Sahu (2003). The first investigates 6 and the second 17 events. Most of the events studied by those groups are rather bright and neither of the above studies specifically targeted the microlensing sources in the Sgr dwarf galaxy. An example of 136.27650.2370/142.27650.6057, which is not a Sgr member, shows that spectroscopic follow-up is essential. Event 136.27650.2370/142.27650.6057 is in our candidate list

<sup>4</sup>Ideally, one would like to perform such a radial velocity test for all microlensing candidates from all microlensing surveys, especially the ones with negative Galactic latitude  $b$ . Due to the location of the MACHO fields, the MACHO data are the most suitable for the search for events with Sgr sources.

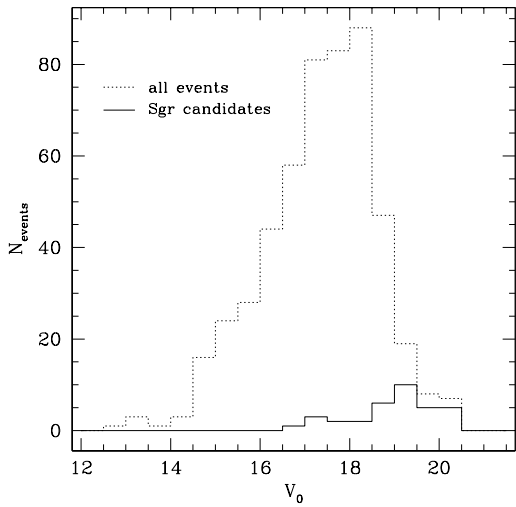


Fig. 4.— The histogram of  $V_0$  magnitudes for a set of all 511 unique microlensing events and 34 Sagittarius candidates. The difference in magnitude distribution is very significant.

but was measured by Cavallo et al. (2002) to have the radial velocity of  $60 \pm 2 \text{ km s}^{-1}$ , inconsistent with the velocity of Sgr dwarf. On the other hand, there may be Sagittarius events hiding among bulge events closer to the Galactic plane. Cook et al. (2004) claim a detection of two likely Sgr events that are distinct through their radial velocity, metallicity and location on the  $(K, J - K)$  CMD. Determination of radial velocities of our candidate Sgr events asks for observations on an 8m class telescope. Unfortunately, these observations cannot be sped up with currently available multi-object instruments, because the candidate Sgr events are distributed over a large area. Their spatial distribution is shown in Figure 5.

As many as five methods to identify Sagittarius events are discussed by Popowski (2004)<sup>5</sup>.

## 8. Statistical properties of the events

### 8.1. Clustering of microlensing events

Figure 2 shows the position of the events on the sky. The events are noticeably concentrated toward the Galactic center and toward the Galactic plane as expected. Examination of the figure

---

<sup>5</sup>See: <http://www.stelab.nagoya-u.ac.jp/hawaii/Popowski/hawaii2004.html>.

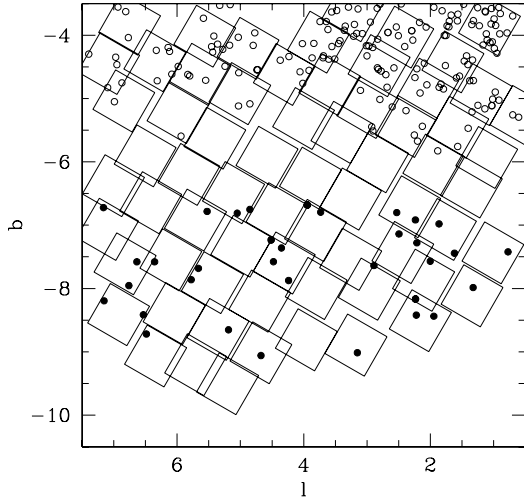


Fig. 5.— Spatial distribution of events (dots) in the MACHO fields (squares) most distant from the Galactic plane. The filled dots represent Sgr candidates. The strip of empty fields at  $b \approx -6$  is caused by very low detection efficiency in those fields and unrelated to the existence of different event populations.

shows some apparent clustering of events on the sky, in particular in fields 108, 104, and 113. If microlensing events are clustered on the sky above random chance it has important consequences. It could indicate clustering of lenses, perhaps in some bound Galactic substructure. We tested for the significance of the clustering in our data by simulating 10000 microlensing experiments each of which found 318 criteria “c” selected unique microlensing events (as in the current data set). The Monte Carlo is described in more detail in the companion paper (Popowski et al. 2004). The result is that we find no strong evidence for clustering beyond random chance. The probability of finding by chance a cluster of 3 events as dense as in the data is between 7 and 36% depending on the assumed optical depth gradient. The chance of finding a 4-event cluster as dense as in the data varies between 4 and 32% depending on the assumed optical depth gradient.

## 8.2. Impact Parameters

One test of microlensing is the distribution of impact parameters,  $u_{\min}$ . The impact parameter  $u_{\min}$  is the distance of closest approach between the lens and the source in units of the Einstein ring radius, and it is completely determined by the maximum magnification. If the efficiency were

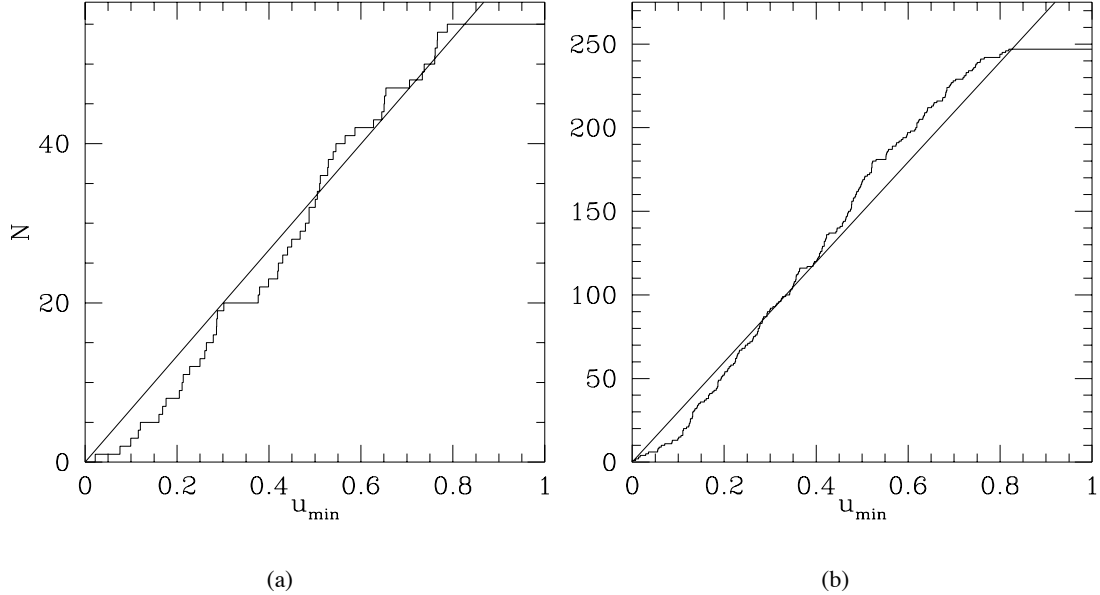


Fig. 6.— Cumulative distribution of impact parameter for clump events (a) and non-clump, selection criteria “c” events (b).

independent of the magnification one would expect a uniform distribution of  $u_{\min}$ 's since every impact parameter is equally likely. In that case, a cumulative distribution of impact parameters should be a straight line from 0 up to the maximum impact parameter allowed by our cuts (the cut  $A_{max} >= 1.5$  corresponds to  $u_{\min} < 0.826$ .) In Figure 6, we plot the cumulative distributions of impact parameters for unique, non-binary events selected by the “c” criteria for both clump giants events (55 events) and non-clump events (247 events). In both cases no correction is made for microlensing efficiency, though this correction is made (with little effect) for the clump giant events in the companion paper (Popowski et al. 2004).

For the clump events, the resulting Kolmogorov-Smirnov (KS) statistic shows excellent agreement with the microlensing hypothesis:  $D = 0.103$  with 55 events, with a probability of 58.0% to find a value of  $D$  this large or larger. For the non-clump events, the agreement is marginal:  $D = 0.095$  with 247 events, for a probability of 2.1% of finding a value of  $D$  this large. This deviation from uniformity can be caused by blending (which can lower the measured maximum amplification and therefore increase the measured  $u_{\min}$ ), by a lower efficiency at larger impact parameter, or by inclusion of non-microlensing events in the sample.

### 8.3. Distributions

Figure 7 shows the distribution of lensing durations  $\hat{t}$  for both the clump giant and non-clump events. Only grade A and B events are included. The average value of  $\hat{t}$  for the non-clump sample is 49 with a standard deviation of 62 days. For comparison note that the clump giant events have a mean  $\hat{t}$  of 56 days with a standard deviation of 64 days. Because the distributions are not Gaussian we also give the median and quartiles for non-clump A and B events 31.1, 17.4, & 57.0, and clump events 30.8, 15.9, & 60.9. These results are consistent with partial blending of the non-clump sample discussed in § 6 but they do not provide any additional support for this hypothesis.

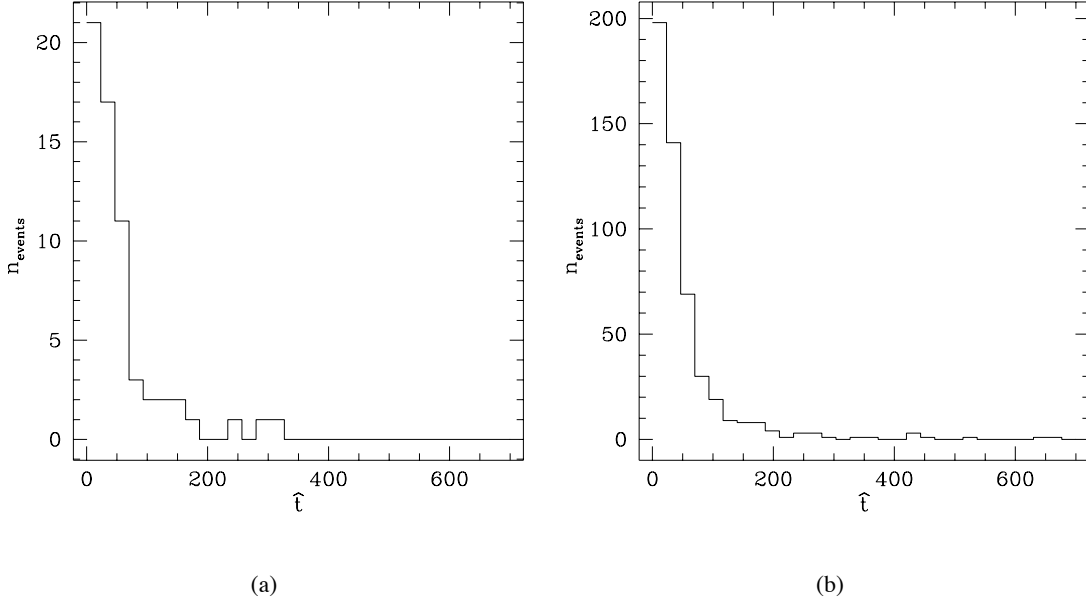


Fig. 7.— Distribution of event durations for clumps giants (a) and non-clumps (b).

Figure 8 shows the distribution of the times of microlensing peaks, mostly showing when observations took place, but is consistent with uniformity when this is taken into account. Figure 9 shows the CMD of the microlensing events, which, as expected, is a reasonable sample of the CMD of the Galactic bulge. The location on a CMD is used in the companion paper to select clump giants.

## 9. Conclusions

In conclusion, light curves and parameters of 528 microlensing events found by the Macho Project (1993-1999) are presented. Included are 5 events on variable stars, 17 binary events, 24 potential binary events, and 1 extended source event. Also included is a representative sample of 36 contaminant events, consisting of 16 cataclysmic variables, and 20 duplicate events. In addition we select 37 (34 unique) events that are potentially lensed Sagittarius sources. The sample of over 500 events presented here is effected significantly by blending and should not be used for quantitative studies without a proper accounting for blending. We present light curves for all 564 microlensing and non-microlensing events. Data and figures will be available at <http://wwwmacho.mcmaster.ca> upon acceptance of this paper.

This work was performed under the auspices of the U.S. Department of Energy, National Nuclear Security Administration by the University of California, Lawrence Livermore National Laboratory under contract No. W-7405-Eng-48. KG and CT were supported in part by the DoE under grant DEFG0390ER40546. DM is supported by FONDAP Center for Astrophysics 15010003.

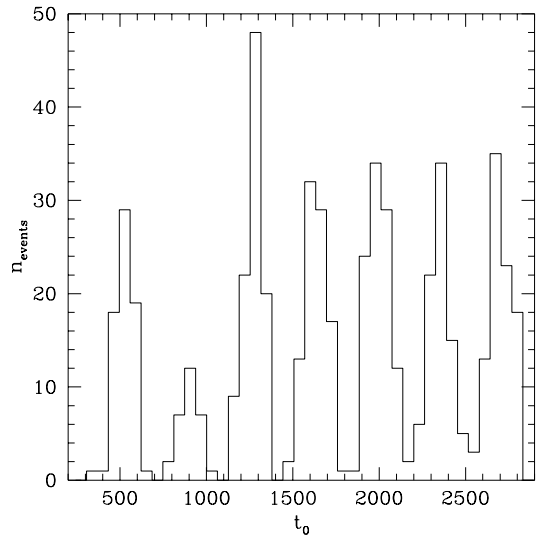


Fig. 8.— Histogram of  $t_0$  of events. The peaks and troughs are due to the lack of observations from November through February. The small number of events in the second year is due to fewer observations in that period.

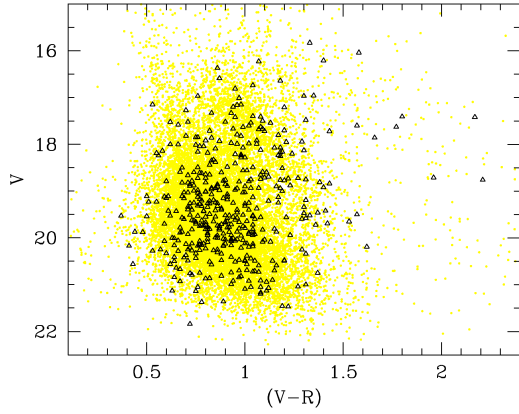


Fig. 9.— Color-magnitude diagram of events (black triangles) and a representative sample of all stars in our fields.

Table 1. Data on the 94 bulge fields.

field	<i>l</i>	<i>b</i>	$\frac{n_{stars}}{100}$	$\frac{n_{clumps}}{100}$	<i>n<sub>events</sub></i>	<i>n<sub>exposures</sub></i>	$\epsilon(50days.)$	$\epsilon(200days)$
101	3.73	-3.02	6284	629.5	30	804	0.41	0.61
102	3.77	-4.11	6545	444	15	421	0.24	0.46
103	4.31	-4.62	6349	368	5	331	0.21	0.36
104	3.11	-3.01	5813	652	28	1639	0.40	0.59
105	3.23	-3.61	6375	539	21	640	0.39	0.52
106	3.59	-4.78	6648	346	0	12	< 0.003	< 0.003
107	4.00	-5.31	6159	269	0	51	0.007	< 0.003
108	2.30	-2.65	6498	790	32	1031	0.49	0.75
109	2.45	-3.20	6926	661	19	761	0.35	0.60
110	2.81	-4.48	6649	408	11	650	0.32	0.57
111	2.99	-5.14	6036	298	5	305	0.21	0.34
112	3.40	-5.53	5147	246.5	0	43	< 0.003	< 0.003
113	1.63	-2.78	6252	834	31	1127	0.51	0.72
114	1.81	-3.50	6665	617	20	776	0.39	0.59
115	2.04	-4.85	5756	325.5	9	357	0.24	0.35
116	2.38	-5.44	5812	268.5	4	314	0.21	0.38
117	2.83	-6.00	5185	198	0	39	0.006	< 0.003
118	0.83	-3.07	6347	741.5	29	1053	0.44	0.74
119	1.07	-3.83	7454	542.5	27	1815	0.45	0.68
120	1.64	-4.42	5599	394	9	676	0.35	0.54
121	1.20	-4.94	5855	344	10	352	0.22	0.37
122	1.57	-5.45	4890	266	3	186	0.15	0.23
123	1.95	-6.05	5119	210.5	1	40	0.006	< 0.003
124	0.57	-5.28	5716	265.5	3	337	0.22	0.39
125	1.11	-5.93	5839	189	1	287	0.21	0.37
126	1.35	-6.40	4789	182	0	36	< 0.003	< 0.003
127	0.28	-5.91	4975	192	0	178	0.13	0.24
128	2.43	-4.03	6160	516.5	9	711	0.35	0.55
129	4.58	-5.93	5123	234.5	0	31	0.006	< 0.003
130	5.11	-6.49	4864	169.5	2	20	0.02	0.02
131	4.98	-7.33	4256	130	1	106	0.12	0.22
132	5.44	-7.91	4533	102	2	180	0.17	0.33
133	6.05	-8.40	4174	70.5	0	176	0.15	0.17
134	6.34	-9.07	3370	46.5	1	197	0.08	0.14
135	3.89	-6.26	5476	179	0	30	0.004	< 0.003
136	4.42	-6.82	5623	137.5	1	207	0.17	0.25
137	4.31	-7.60	4488	101	4	193	0.15	0.36

Table 1—Continued

field	<i>l</i>	<i>b</i>	$\frac{n_{stars}}{100}$	$\frac{n_{clumps}}{100}$	<i>n<sub>events</sub></i>	<i>n<sub>exposures</sub></i>	$\epsilon(50days.)$	$\epsilon(200days)$
138	4.69	−8.20	4380	95.5	0	201	0.16	0.21
139	5.35	−8.65	4112	81	1	191	0.11	0.10
140	5.71	−9.20	3723	64	0	209	0.12	0.24
141	3.26	−6.59	5001	159	0	28	0.03	0.02
142	3.81	−7.08	4985	126.5	2	218	0.15	0.35
143	3.80	−8.00	4767	97	0	210	0.17	0.25
144	4.68	−9.02	3798	50.5	1	210	0.10	0.18
145	5.20	−9.50	3385	49.5	1	210	0.12	0.23
146	3.26	−7.54	3798	106	0	207	0.19	0.33
147	3.96	−8.81	4135	66	0	208	0.19	0.20
148	2.33	−6.71	5824	161.5	2	229	0.18	0.30
149	2.43	−7.43	4042	112.5	2	236	0.19	0.34
150	2.96	−8.01	4474	98.5	1	229	0.18	0.28
151	3.17	−8.89	3432	85	1	194	0.14	0.23
152	1.76	−7.07	4995	124	2	235	0.22	0.31
153	2.11	−7.87	4763	85.5	3	231	0.16	0.35
154	2.16	−8.51	3936	82	3	247	0.19	0.20
155	1.01	−7.44	4481	95.5	1	247	0.17	0.36
156	1.34	−8.12	4660	88.5	1	249	0.13	0.32
157	0.08	−7.76	3822	105.5	0	258	0.20	0.37
158	7.08	−4.44	4703	246.5	4	260	0.20	0.29
159	6.35	−4.40	5890	258.5	6	464	0.27	0.46
160	6.84	−5.04	4940	248	1	208	0.15	0.26
161	5.56	−4.01	5878	366	6	467	0.32	0.45
162	5.64	−4.62	5914	301	5	382	0.22	0.38
163	5.98	−5.22	5311	259	2	251	0.19	0.36
164	6.51	−5.90	4901	167.5	0	20	0.002	< 0.003
165	7.01	−6.38	4349	135	0	14	< 0.003	< 0.003
166	7.10	−7.07	4175	131.5	1	110	0.09	0.14
167	4.88	−4.21	6268	388.5	5	364	0.26	0.40
168	5.01	−4.92	4724	298	3	210	0.17	0.26
169	5.40	−5.63	4896	208	0	24	0.004	< 0.003
170	5.81	−6.20	4886	170	0	17	< 0.003	< 0.003
171	6.42	−6.65	4834	120.5	0	125	0.15	0.19
172	6.82	−7.61	4036	89	2	132	0.13	0.17
173	6.92	−8.41	3532	87	1	146	0.06	0.09
174	5.71	−6.92	4979	143.5	1	144	0.18	0.22

Table 1—Continued

field	<i>l</i>	<i>b</i>	$\frac{n_{stars}}{100}$	$\frac{n_{clumps}}{100}$	<i>n<sub>events</sub></i>	<i>n<sub>exposures</sub></i>	$\epsilon(50days.)$	$\epsilon(200days)$
175	6.10	−7.55	4173	111.5	1	97	0.06	0.10
176	2.93	−2.30	7741	814.5	10	423	0.25	0.43
177	6.75	−3.82	5950	319	3	416	0.30	0.43
178	5.24	−3.42	8186	477	7	376	0.27	0.41
179	4.92	−2.83	7159	510	10	349	0.20	0.39
180	5.93	−2.69	6388	478	6	343	0.21	0.38
301	18.77	−2.05	5608	—	6	925	0.31	0.46
302	18.09	−2.24	5175	—	3	365	0.28	0.37
303	17.30	−2.33	4029	—	0	369	0.22	0.40
304	9.07	−2.70	5080	—	6	458	0.30	0.50
305	9.69	−2.36	4628	—	3	411	0.29	0.46
306	8.46	−3.03	5886	—	3	423	0.28	0.40
307	7.84	−3.37	6565	—	4	435	0.27	0.43
308	10.02	−2.98	5038	—	2	360	0.26	0.40
309	9.40	−3.31	5494	—	1	347	0.23	0.39
310	8.79	−3.64	6488	—	10	387	0.26	0.42
311	8.17	−3.97	7514	—	10	396	0.28	0.39
401	2.02	−1.93	6630	964.5	17	429	0.25	0.45
402	1.27	−2.09	7098	1153	29	1256	0.26	0.45
403	0.55	−2.32	6798	1085	24	473	0.26	0.45

Note. — Efficiencies (columns 8 and 9) are averaged over  $A_{max}$ . The classification of stars as clump giants is expected to be very difficult in 300 series fields, so we refrain from quoting specific numbers for these fields.

Table 2. Selection Criteria

Selection	Description
<b>microlensing fit parameter cuts:</b>	
$N_{(V-R)} > 0$	require color information
$\chi^2_{out} < 3.0, \chi^2_{out} > 0.0$	require high quality baselines
$N_{amp} \geq 8$	require 8 points in the amplified region
$N_{rising} \geq 1, N_{falling} \geq 1$	require at least one point in the rising and falling part of the peak
$A_{max} > 1.5$	magnification threshold
$(A_{max} - 1) > 2.0(\sigma_R + \sigma_B)$	signal to noise cut on amplification
$(\sigma_R + \sigma_B) < (0.05 \delta\chi^2) / (N_{amp} \chi^2_{in} \chi^2_{out})$	$\left. \begin{array}{l} (N_{amp} \chi^2_{out} f_{chrom}) / (befaft \delta\chi^2) < 0.0003 \\ (N_{amp} \chi^2_{in}) / (befaft \delta\chi^2) < 0.00004 \end{array} \right\}$ remove spurious photometric signals caused by nearby saturated stars
$\delta\chi^2 / fc2 > 320.0$	
$\delta\chi^2 / \chi^2_{peak} \geq 400.0$	
$0.5(rcrda + bcrda) \leq 143.0$	good overall fit to microlensing lc shape
$\xi_B^{auto} / \xi_R^{auto} < 2.0$	same quality fit in peak as whole lc
$t_0 > 419.0, t_0 < 2850.0$	source star not too crowded
$\hat{t} < 1700$	remove long period variables
<b>clump giant cuts:</b>	
$V \geq 15, V \leq 20.5$	constrain the peak to period of observations
$V \geq 4.2(V - R) + 12.4$	limit event duration to $\sim$ half the span of observations
$V \leq 4.2(V - R) + 14.2$	
$(V - R) \geq (V - R)_{boundary}$	
exclude fields 301 – 311	

Table 3. Event Parameters

field.tile.seq	$\alpha$ (2000)	$\delta$ (2000)	$V$	$V - R$	$t_0$	$\hat{t}$	$A_{max}$	$\frac{\chi^2}{n_{dof}}$	Gr.	Sel.	Notes
101.20650.1216 <sup>a</sup>	18 04 20.25	-27 24 45.3	18.01	0.67	1971.8	10.3	2.19	1.09	A	cb	bin
101.20658.2639	18 04 22.39	-26 53 15.3	20.73	0.97	1204.7	22.3	7.66	0.84	A	c	
101.20908.1433	18 04 57.68	-27 33 18.4	18.57	0.82	1598.6	14.1	1.41	0.46	C	a	bin
101.20910.2922 <sup>b</sup>	18 04 54.54	-27 25 50.0	19.43	0.74	2265.9	243	9.12	1.03	A	c	
101.20913.2158	18 04 56.18	-27 13 40.0	19.56	0.92	2484.9	57.0	4.91	0.88	B	a	
101.20914.3873	18 04 56.32	-27 10 41.3	20.06	0.94	2008.8	33.8	1.85	1.74	B	c	
101.21042.5059 <sup>c</sup>	18 05 28.27	-27 16 21.3	20.14	0.84	2805.4	44.0	4.45	0.73	B	c	
101.21045.2528	18 05 12.63	-27 05 47.1	19.29	0.69	2426.3	19.2	4.82	0.80	B	ab	bin
101.21170.2699	18 05 48.16	-27 24 16.4	18.88	0.71	2807.3	11.4	4.22	0.79	B	a	
101.21171.4799	18 05 38.16	-27 23 07.8	20.20	1.00	1599.4	14.5	2.04	1.04	B	c	bin
101.21174.1990	18 05 39.23	-27 08 53.8	18.86	0.72	1356.7	9.67	2.72	1.12	B	e	
101.21174.2534 <sup>d</sup>	18 05 38.71	-27 08 30.0	19.17	0.78	1909.2	15.3	1.83	0.75	B	e	
101.21176.5465	18 05 31.60	-27 03 11.5	21.12	0.75	2426.1	16.6	3.37	0.93	B	e	
101.21307.880	18 06 05.20	-26 59 38.3	20.32	0.86	537.8	53.4	8.10	0.86	A	c	
101.21428.2452	18 06 21.15	-27 33 57.8	19.07	0.75	2751.2	36.4	2.09	1.15	B	c	bin
101.21437.2090	18 06 20.53	-26 58 39.6	19.21	0.91	611.5	42.1	2.16	1.07	B	c	
101.21437.2192	18 06 23.82	-26 58 54.3	19.01	0.81	2384.7	30.8	1.91	1.44	A	c	
101.21558.2113	18 06 37.58	-27 35 40.1	19.00	0.74	553.9	12.6	56.1	1.23	A	c	
101.21561.5337	18 06 25.89	-27 22 47.7	20.39	0.76	2669.0	17.2	3.64	1.12	B	c	
101.21564.4657	18 06 28.73	-27 09 35.6	20.52	0.98	1230.2	17.2	7.66	1.02	A	c	
101.21689.2648	18 06 54.84	-27 29 21.8	19.27	0.84	2370.6	53.7	1.46	0.75	C	e	
101.21689.315 <sup>f</sup>	18 06 58.30	-27 27 45.8	17.51	1.10	593.5	165	4.80	1.19	A	c	
101.21691.836	18 06 52.73	-27 23 18.9	17.28	0.70	1212.3	30.4	2.01	0.35	A	c	
101.21821.128	18 07 04.26	-27 22 06.3	16.24	1.37	1321.2	68.3	23.5	25.8	A	e	
101.21948.3692	18 07 23.42	-27 35 28.8	20.87	0.90	2408.0	17.2	3.78	0.79	B	e	
101.21949.2465	18 07 32.65	-27 31 35.6	19.92	0.86	579.9	34.4	6.00	1.40	A	c	
101.21950.1897	18 07 24.99	-27 24 40.5	19.27	0.78	1249.1	5.74	1.60	0.92	B	c	
101.21950.861	18 07 20.78	-27 24 09.7	18.48	0.90	1340.7	24.7	2.64	0.41	A	c	
102.22466.140 <sup>f</sup>	18 08 47.04	-27 40 47.3	16.81	0.95	1275.6	153	3.88	0.95	A	c	
102.22598.2894	18 09 00.08	-27 35 38.9	19.72	0.84	2688.8	15.5	1.51	1.30	C	e	
102.22725.1408	18 09 13.53	-27 45 45.0	19.27	0.94	1916.9	121	1.81	0.57	B	c	
102.22851.2409	18 09 44.70	-28 00 58.6	19.64	0.96	2368.4	40.2	2.32	0.96	B	c	
102.22851.4872 <sup>e</sup>	18 09 30.68	-28 00 48.8	20.21	0.74	1307.7	18.0	3.38	0.84	B	e	$R \neq B$
102.23112.1759	18 10 09.43	-27 56 45.7	19.41	0.76	1977.7	27.1	5.04	1.23	A	c	
102.23246.5046	18 10 34.52	-27 40 24.5	20.28	0.63	2715.1	9.21	3.62	1.09	B	e	
102.23370.476	18 10 50.72	-28 04 47.6	18.09	0.86	2010.1	25.4	1.70	1.07	A	c	bin
102.23379.2909	18 10 58.82	-27 31 01.6	19.71	0.80	1693.0	45.5	2.19	0.68	B	c	
102.23501.4570	18 11 03.79	-27 59 58.8	20.16	0.84	2684.2	55.7	1.93	1.44	C	a	bin
102.23503.2521	18 11 10.12	-27 54 34.3	19.64	0.85	454.3	74.3	5.40	0.76	A	c	
102.23503.4283	18 11 01.59	-27 53 59.0	19.82	0.80	2335.4	29.3	2.98	0.64	B	c	
102.23635.1426	18 11 32.49	-27 45 27.0	18.82	0.69	1282.9	62.6	4.16	1.04	A	c	
103.24024.1785	18 12 26.00	-27 48 37.8	19.04	0.70	2318.9	98.0	1.34	0.83	B	e	

Table 3—Continued

field.tile.seq	$\alpha$ (2000)	$\delta$ (2000)	$V$	$V - R$	$t_0$	$\hat{t}$	$A_{max}$	$\frac{\chi^2}{n_{dof}}$	Gr.	Sel.	Notes
103.24030.3425	18 12 14.65	−27 25 39.0	19.57	0.70	2004.5	16.1	3.78	1.12	A	c	
103.24161.2085	18 12 45.87	−27 20 04.4	19.15	0.69	2730.5	50.0	3.43	0.99	A	c	
103.24286.768	18 12 49.71	−27 41 42.6	18.19	0.82	2064.0	77.0	1.36	2.38	B	e	
103.24544.794	18 13 27.58	−27 49 11.6	19.80	0.81	2065.0	58.4	1.70	0.89	B	a	
104.19990.4674	18 03 00.48	−28 04 45.7	18.30	0.78	1175.2	53.9	1.63	1.25	C	e	
104.19992.858 <sup>†</sup>	18 02 53.82	−27 57 50.0	18.60	1.08	1169.7	106	2.23	2.15	A	c	
104.20119.6312 <sup>f†</sup>	18 03 20.75	−28 08 14.5	18.02	1.09	1975.3	38.7	1.62	1.62	A	c	
104.20121.1692	18 03 15.25	−28 00 14.1	18.62	0.89	1986.1	166	2.54	0.97	A	c	
104.20121.2255	18 03 09.05	−28 01 45.3	19.34	1.01	480.5	34.6	3.62	0.42	A	c	
104.20251.1117 <sup>†</sup>	18 03 29.02	−28 00 31.0	18.23	0.98	463.2	45.5	2.09	0.93	A	c	
104.20251.50 <sup>†</sup>	18 03 34.05	−28 00 18.9	17.34	0.93	493.9	287	10.1	1.75	A	c	
104.20259.572 <sup>†</sup>	18 03 33.39	−27 27 47.3	18.17	1.20	538.5	14.2	1.58	1.56	A	c	
104.20382.803 <sup>†</sup>	18 03 53.19	−27 57 35.7	17.80	0.96	1765.8	254	5.72	4.40	A	c	
104.20387.2071	18 03 51.43	−27 37 40.2	19.04	0.72	2093.4	12.8	1.64	1.79	A	e	
104.20388.2766	18 03 53.97	−27 33 30.5	19.83	1.01	1691.5	75.5	7.70	0.6	A	c	bin
104.20514.1500	18 04 06.08	−27 48 26.3	18.95	1.09	1993.0	2.58	15.1	1.03	C	a	
104.20515.498 <sup>†</sup>	18 04 09.66	−27 44 35.1	17.66	1.00	2061.7	53.6	1.76	1.42	A	c	
104.20640.8423 <sup>g†</sup>	18 04 33.65	−28 07 31.9	17.16	0.97	2374.9	30.8	1.65	2.23	A	c	
104.20645.3129 <sup>†</sup>	18 04 26.17	−27 47 35.1	17.69	1.07	1558.3	152	1.82	0.77	A	c	
104.20775.2644	18 04 50.73	−27 45 57.3	20.02	0.92	1899.9	46.3	5.42	0.92	A	c	
104.20779.9616	18 04 54.08	−27 30 07.0	20.03	0.94	2678.6	37.4	1.74	0.94	B	e	
104.20904.3155	18 05 07.31	−27 51 11.4	19.95	0.97	1310.4	33.5	2.41	0.94	A	c	
104.20906.3973	18 05 02.50	−27 42 17.2	19.93	0.83	1738.6	654	2.05	1.85	B	a	bin
104.20910.7700 <sup>b</sup>	18 04 54.54	−27 25 49.8	19.34	0.85	2266.2	211	8.64	0.93	A	c	
104.21032.4118	18 05 15.42	−27 58 25.0	19.87	0.73	1620.1	29.3	2.50	0.92	A	c	
104.21161.1997 <sup>h</sup>	18 05 34.45	−28 02 51.8	18.66	0.81	1301.7	37.5	7.66	1.02	A	c	
104.21162.3642 <sup>i</sup>	18 05 47.75	−27 56 32.2	19.70	0.87	1694.6	71.6	1.76	1.59	C	c	
104.21164.4093 <sup>j</sup>	18 05 41.42	−27 51 03.1	20.07	0.97	1601.8	33.8	1.77	0.71	B	e	
104.21293.1164 <sup>k</sup>	18 06 03.99	−27 55 05.0	17.83	0.71	1294.0	37.2	1.61	0.63	B	c	bin
104.21421.131 <sup>ae</sup>	18 06 08.65	−28 00 22.4	17.78	0.85	2640.8	7.54	2.61	20	A	c	
104.21423.530 <sup>l</sup>	18 06 09.10	−27 53 38.7	19.77	0.78	1634.1	37.3	1.77	1.49	B	c	
105.21161.7671 <sup>h</sup>	18 05 34.44	−28 02 51.2	18.79	0.76	1301.7	39.2	8.16	0.94	A	c	
105.21162.7174 <sup>i</sup>	18 05 47.79	−27 56 32.6	19.77	0.86	1695.7	61.2	1.72	2.04	B	c	
105.21164.9983 <sup>j</sup>	18 05 41.46	−27 51 03.3	20.14	0.85	1601.2	37.2	1.83	0.82	B	c	
105.21287.3893	18 05 49.89	−28 17 19.5	20.25	0.99	2082.9	21.6	2.79	0.97	C	e	
105.21293.6550 <sup>k</sup>	18 06 04.01	−27 55 04.9	17.90	0.71	1295.7	28.3	1.71	0.63	B	c	
105.21417.101	18 06 11.95	−28 16 52.8	16.22	1.08	1540.7	108	1.91	16.6	A	ab	bin
105.21422.1228	18 06 20.41	−27 56 13.4	17.94	0.88	2256.9	75.2	2.80	2.93	A	e	
105.21423.5762 <sup>l</sup>	18 06 09.11	−27 53 38.6	19.90	0.79	1636.8	40.2	1.84	0.75	B	c	
105.21425.3499	18 06 08.51	−27 46 13.2	19.11	0.91	1361.5	24.8	2.77	0.95	B	e	
105.21681.2244	18 06 53.94	−28 01 16.5	19.36	0.75	2665.4	9.31	1.54	0.85	C	e	$R \neq B$
105.21807.4900	18 07 18.17	−28 17 38.4	20.94	1.11	2013.9	9.27	3.83	0.80	B	e	

Table 3—Continued

field.tile.seq	$\alpha$ (2000)	$\delta$ (2000)	$V$	$V - R$	$t_0$	$\hat{t}$	$A_{max}$	$\frac{\chi^2}{n_{dof}}$	Gr.	Sel.	Notes
105.21813.2516 <sup>†</sup>	18 07 07.07	-27 52 34.3	17.41	1.08	1928.5	17.5	13.2	1.14	A	c	
105.22075.1451	18 07 43.89	-27 44 22.0	18.91	0.87	1220.2	17.4	1.61	0.59	B	c	
105.22200.1712	18 07 59.87	-28 05 24.6	19.24	0.86	2272.4	22.9	2.03	1.25	B	e	
105.22206.366	18 08 00.21	-27 40 52.8	19.53	1.54	1654.3	49.6	2.08	1.52	B	e	
105.22327.3556	18 08 17.90	-28 16 16.6	19.60	0.68	1620.5	22.6	2.30	0.90	A	c	
105.22329.1480	18 08 28.56	-28 11 20.7	19.67	0.62	539.8	126	8.07	5.59	A	c	bin
105.22332.2555	18 08 25.19	-27 58 38.2	19.25	1.15	1210.1	137	1.84	0.75	A	c	
105.22459.1549	18 08 46.10	-28 10 08.6	19.42	1.02	2116.3	20.9	2.35	1.15	B	c	
105.22462.5692	18 08 42.71	-27 59 39.6	19.84	0.89	535.5	140	3.12	0.59	C	e	bin
108.18558.329	17 59 41.85	-28 12 10.3	19.50	0.98	1362.2	83.7	2.11	2.16	A	c	
108.18559.526	17 59 42.21	-28 08 41.5	20.13	1.01	1279.1	23.7	2.94	1.35	B	c	
108.18685.3171	18 00 01.28	-28 27 41.2	19.90	1.16	580.6	42.8	2.88	0.66	A	c	
108.18686.3423	17 59 56.61	-28 23 01.9	19.84	0.95	2667.8	23.4	2.53	0.6	A	c	
108.18689.1979	17 59 49.63	-28 10 56.4	19.05	1.00	976.3	20.5	3.60	2.05	A	c	var
108.18943.3744 <sup>m</sup>	18 00 21.61	-28 32 01.2	19.23	0.84	2270.7	50.2	3.12	0.68	B	c	
108.18947.3618 <sup>†</sup>	18 00 29.14	-28 19 20.3	17.73	1.10	1287.9	45.6	2.05	0.94	A	c	
108.18951.1221 <sup>†</sup>	18 00 25.87	-28 02 35.2	18.93	1.19	583.6	45.8	2.16	0.92	A	c	
108.18951.593 <sup>†</sup>	18 00 33.78	-28 01 10.5	18.08	1.18	1991.6	47.3	4.05	7.02	A	cb	bin
108.18952.941 <sup>†</sup>	18 00 36.05	-27 58 30.0	18.92	1.17	1324.9	66.9	2.39	1.11	A	c	
108.19073.2291	18 00 39.56	-28 34 43.8	...	...	1975.1	57.6	1.41	0.42	B	b	bin
108.19074.550 <sup>†</sup>	18 00 52.24	-28 29 52.0	17.55	1.03	2050.6	9.26	1.78	0.97	A	c	
108.19082.1466	18 00 39.34	-27 58 34.9	19.25	1.02	1681.4	48.4	1.76	0.40	B	e	
108.19082.3434	18 00 49.97	-27 58 45.1	20.54	1.02	2033.6	43.9	1.75	0.72	B	a	
108.19204.267	18 01 07.72	-28 31 41.4	16.74	1.04	2678.5	39.9	2.28	0.81	A	c	
108.19204.2857	18 01 10.52	-28 31 22.2	19.39	0.89	533.2	44.9	1.63	1.23	C	e	
108.19211.3382	18 01 13.75	-28 01 24.7	19.85	0.83	1359.4	17.8	3.95	0.49	B	e	
108.19212.869	18 01 09.01	-27 57 58.8	18.38	0.85	1636.9	80.3	6.94	0.83	A	c	
108.19333.1878	18 01 21.18	-28 32 39.4	17.33	0.98	1937.0	73.3	1.82	3.28	A	b	bin
108.19333.4264	18 01 30.83	-28 32 17.0	19.81	1.09	2012.1	7.99	1.61	0.70	B	c	
108.19334.1583 <sup>†</sup>	18 01 26.31	-28 31 14.0	17.68	0.96	1231.4	18.5	4.09	0.38	A	c	
108.19337.417	18 01 24.41	-28 17 32.9	18.57	0.99	2769.5	83.3	1.51	0.92	A	c	
108.19341.1936 <sup>n</sup>	18 01 28.55	-28 02 13.9	19.92	1.02	2356.0	61.4	7.08	0.68	A	c	
108.19464.254	18 01 33.95	-28 28 02.2	16.98	1.30	2086.7	58.1	1.70	10	A	c	
108.19464.5201	18 01 38.88	-28 30 03.4	20.45	0.73	1974.5	36.2	3.21	0.54	A	c	
108.19466.2869	18 01 47.14	-28 21 25.8	19.30	0.91	1306.6	21.8	1.40	0.83	C	e	
108.19595.2757	18 02 09.89	-28 26 03.8	19.27	0.86	572.8	22.7	18.0	0.65	A	c	
108.19599.1605	18 01 57.09	-28 08 05.3	19.12	1.17	1347.1	68.8	8.46	1.12	A	c	
108.19602.2404	18 01 59.16	-27 56 32.9	19.61	1.00	2757.1	49.0	1.55	1.30	C	a	
108.19602.415	18 01 59.72	-27 57 21.6	18.82	2.25	1909.5	92.5	4.32	12.3	B	e	var
108.19853.8058 <sup>o</sup>	18 02 29.01	-28 33 12.0	19.15	0.88	2289.4	35.4	2.01	0.64	A	c	
108.19985.8020	18 02 46.97	-28 25 39.3	20.17	0.86	1661.4	28.1	1.82	1.36	C	e	
109.19720.3549	18 02 21.89	-28 47 02.4	19.67	1.05	1736.0	9.36	3.40	1.17	B	a	

Table 3—Continued

field.tile.seq	$\alpha$ (2000)	$\delta$ (2000)	$V$	$V - R$	$t_0$	$\hat{t}$	$A_{max}$	$\frac{\chi^2}{n_{dof}}$	Gr.	Sel.	Notes
109.19850.956	18 02 29.06	-28 45 39.0	17.83	0.98	1279.6	60.4	1.42	0.80	A	e	
109.19853.2074 <sup>o</sup>	18 02 29.02	-28 33 12.1	19.13	0.95	2288.8	37.3	1.97	0.64	A	c	
109.19853.4889	18 02 44.36	-28 33 08.9	20.13	0.77	2633.6	14.1	2.45	0.70	B	e	
109.19858.3675	18 02 31.34	-28 12 20.6	19.50	0.85	2297.6	17.5	1.59	1.14	C	e	
109.19986.2444 <sup>p</sup>	18 03 01.11	-28 21 08.6	19.07	0.77	1258.4	43.8	1.80	0.56	B	c	
109.19987.2565	18 02 55.86	-28 16 55.9	18.94	0.83	1947.6	9.90	2.31	1.63	A	c	
109.20118.5042	18 03 15.48	-28 15 23.7	20.20	0.90	2231.5	47.9	14.7	1.38	C	a	
109.20119.1051 <sup>f†</sup>	18 03 20.74	-28 08 14.5	18.11	0.97	1977.6	28.7	1.62	1.01	A	c	
109.20246.4248	18 03 24.69	-28 20 22.4	19.86	0.90	1304.6	58.6	2.08	0.87	A	c	
109.20370.5166 <sup>q</sup>	18 03 58.75	-28 47 38.0	20.79	0.96	2787.6	22.0	5.87	0.94	A	c	
109.20379.2012	18 03 59.42	-28 10 35.5	20.57	0.83	1262.0	85.9	2.21	0.69	A	c	
109.20635.2121	18 04 18.66	-28 25 43.1	19.57	0.76	2544.5	707	1.77	2.12	C	c	
109.20635.2193	18 04 34.45	-28 25 33.5	19.53	0.77	1359.1	38.5	1.84	0.63	A	c	
109.20640.360 <sup>g†</sup>	18 04 33.66	-28 07 32.5	17.33	1.05	2375.1	28.7	1.67	0.72	A	c	
109.20893.3423	18 05 05.28	-28 34 41.7	19.78	0.75	2742.0	265	6.07	1.73	B	c	$R \neq B$
109.21024.5007	18 05 18.03	-28 28 52.9	20.36	0.78	1321.2	116	5.24	1.16	A	c	
110.22194.461	18 08 07.32	-28 31 23.4	18.05	0.78	484.7	11.7	1.84	1.08	A	c	
110.22454.1042	18 08 48.95	-28 31 07.7	18.45	0.81	2624.5	62.5	1.38	1.67	B	e	
110.22455.842 <sup>†</sup>	18 08 51.27	-28 27 11.2	18.28	0.98	1900.1	19.8	2.54	0.84	A	c	
110.22585.1719	18 08 55.39	-28 24 57.7	19.32	0.75	1209.2	52.2	1.87	1.42	A	c	
110.22707.1502	18 09 22.31	-28 57 57.1	18.90	0.74	593.1	9.19	1.53	0.97	B	c	
110.22840.2227	18 09 38.97	-28 46 32.1	18.84	0.71	1263.0	9.25	2.15	0.90	C	e	
110.22844.4168	18 09 32.46	-28 30 06.3	21.94	0.82	506.5	37.4	4.55	0.50	B	c	
110.22969.4258	18 10 01.14	-28 48 44.4	20.14	0.72	2250.8	22.9	3.52	0.84	B	c	
110.22970.4137	18 10 00.26	-28 45 42.0	19.96	0.53	2429.7	19.0	3.00	0.98	B	c	$R \neq B$
110.22970.449	18 09 55.98	-28 44 10.8	19.39	0.87	470.3	10.2	2.32	0.99	A	c	
110.23098.4042	18 10 04.86	-28 54 18.4	20.12	0.79	543.7	30.0	2.57	0.65	B	c	
110.23356.3958	18 10 50.13	-29 00 59.6	19.94	0.81	1163.8	122	1.77	0.70	B	e	
111.23746.772	18 11 51.54	-29 00 34.5	18.02	0.76	2303.0	21.6	1.92	1.50	A	c	
111.23873.4918	18 11 54.95	-29 14 09.0	20.70	0.81	1666.7	23.7	541	1.12	C	e	
111.23881.726	18 11 57.13	-28 40 21.2	18.15	0.87	2331.8	27.7	1.52	0.69	C	a	
111.24655.3092	18 13 52.83	-29 06 02.6	19.52	0.62	1995.8	14.9	2.94	1.05	A	c	
111.24784.884	18 14 06.30	-29 08 56.1	18.26	0.73	1604.4	21.2	1.38	0.63	C	e	bin
113.18156.1823	17 58 43.18	-29 00 28.9	19.55	0.95	1649.0	15.6	2.86	1.13	B	e	
113.18283.3925	17 59 06.16	-29 12 07.3	19.37	0.83	2481.5	23.6	1.41e+9	0.62	B	a	
113.18290.3513	17 58 59.05	-28 44 46.4	19.27	0.65	798.5	27.3	1.86	1.22	C	e	
113.18292.2374	17 59 00.59	-28 36 57.5	19.17	1.04	1193.5	46.1	9.11	0.49	A	c	
113.18414.1512	17 59 14.99	-29 08 12.9	18.06	0.79	910.3	24.0	3.04	1.65	A	c	
113.18414.4153	17 59 16.09	-29 10 35.0	19.39	0.85	636.4	11.7	3.51	0.79	A	c	
113.18415.5194	17 59 19.59	-29 06 07.1	20.32	1.18	1692.7	25.8	2.59	0.84	C	a	
113.18422.3531	17 59 16.72	-28 39 16.7	19.47	0.83	820.0	26.0	1.72	0.90	C	e	
113.18550.1664	17 59 40.61	-28 47 24.5	18.44	0.95	1650.2	36.9	1.81	0.35	A	c	

Table 3—Continued

field.tile.seq	$\alpha$ (2000)	$\delta$ (2000)	$V$	$V - R$	$t_0$	$\hat{t}$	$A_{max}$	$\frac{\chi^2}{n_{dof}}$	Gr.	Sel.	Notes
113.18550.3650	17 59 29.86	-28 43 54.8	19.32	0.72	887.9	6.84	1.75	0.70	B	e	
113.18550.4183	17 59 39.96	-28 43 46.8	21.02	1.82	797.8	42.1	1.67	1.09	C	e	
113.18552.581 <sup>†</sup>	17 59 35.90	-28 36 24.3	17.60	1.02	603.7	27.9	1.77	1.11	B	c	
113.18674.756	17 59 53.40	-29 09 07.8	17.42	0.94	1879.0	114	5.82e+7	3.23	A	b	bin
113.18676.4164	18 00 01.33	-29 02 04.8	19.40	0.82	554.5	13.9	1.57	1.33	C	e	$R \neq B$
113.18680.3511	18 00 01.98	-28 45 17.8	19.36	0.80	1613.8	23.5	3.20	1.18	A	c	
113.18681.4992	17 59 50.67	-28 42 33.1	20.21	0.96	2330.8	20.4	11.6	0.82	B	c	
113.18804.1061 <sup>†</sup>	18 00 03.38	-29 11 04.2	18.30	1.02	1166.6	6.53	1.62	0.96	B	c	
113.18807.1433	18 00 13.15	-28 56 16.8	19.77	0.80	1574.8	26.2	1.89	0.64	B	e	
113.18809.3408	18 00 02.91	-28 51 02.3	19.77	0.90	564.5	16.1	3.71	0.64	A	c	
113.18810.2999 <sup>r</sup>	18 00 06.81	-28 44 00.0	19.33	0.78	2334.2	14.8	2.27	0.52	B	c	
113.18810.4076	18 00 14.08	-28 44 54.5	19.92	0.83	1756.9	34.2	3.44	10	B	e	
113.18812.4511	18 00 03.62	-28 39 14.1	21.02	0.95	1277.6	17.3	3.04	0.88	B	c	
113.18932.2003	18 00 37.45	-29 17 22.5	19.55	0.96	1642.8	11.1	1.59	0.74	B	e	
113.18934.4131	18 00 28.84	-29 09 34.9	19.82	0.82	1183.0	6.31	4.61	0.39	A	c	
113.18940.2606	18 00 37.60	-28 45 22.1	19.16	0.75	861.8	9.73	1.58	0.73	B	e	
113.19064.1665	18 00 44.21	-29 10 32.8	18.95	1.04	949.5	28.7	1.63	0.96	A	c	
113.19066.2168	18 00 54.05	-29 01 08.7	18.96	0.96	533.2	10.4	1.80	1.13	B	e	
113.19192.365 <sup>†</sup>	18 01 06.92	-29 18 53.8	17.80	1.17	2092.6	36.9	1.97	0.52	B	c	
113.19196.3672	18 01 15.02	-29 01 48.4	19.77	0.89	2049.2	10.2	7.94	0.84	A	c	
113.19325.2001	18 01 18.14	-29 05 49.4	19.07	0.90	2285.2	37.7	9.48	0.24	A	c	
114.19583.5176	18 01 59.13	-29 12 41.4	19.58	0.84	2019.6	39.2	8.94	1.87	A	c	
114.19587.3861	18 02 00.22	-28 57 27.4	19.67	0.90	2306.8	21.8	6.07	1.11	A	c	
114.19589.4067	18 02 06.33	-28 50 45.3	18.66	0.83	1371.9	19.1	1.97	0.96	A	c	
114.19589.4149	18 01 58.45	-28 50 07.5	18.65	0.79	2020.2	20.0	1.72	1.24	A	c	
114.19712.1763	18 02 17.96	-29 18 11.3	19.15	0.92	2660.8	9.78	1.40	0.62	B	e	
114.19712.813 <sup>†</sup>	18 02 11.41	-29 19 20.8	18.13	1.09	1643.4	23.7	3.58	0.62	A	c	
114.19846.777 <sup>†</sup>	18 02 36.82	-29 01 42.1	18.00	1.02	545.4	65.0	1.55	1.86	A	c	
114.19970.843 <sup>†</sup>	18 02 54.45	-29 26 29.5	17.99	0.96	1281.9	14.7	4.47	0.65	A	c	
114.20104.617	18 03 16.02	-29 08 20.3	19.12	0.82	2220.4	81.3	1.01e+6	0.75	C	a	
114.20235.908	18 03 39.60	-29 05 38.6	20.12	0.89	2057.6	47.4	1.89	1.11	A	c	
114.20360.1661	18 03 44.17	-29 26 16.9	18.76	0.90	1895.9	25.1	2.63	0.98	A	c	
114.20370.6070 <sup>q</sup>	18 03 58.80	-28 47 38.6	20.47	0.80	2788.0	28.2	6.25	1.59	A	c	
114.20489.3552	18 04 10.63	-29 28 57.8	20.01	0.86	2653.8	6.74	1.85	1.2	B	e	
114.20491.1613	18 04 02.25	-29 21 09.8	18.61	0.69	558.4	19.9	3.83	0.91	A	c	
114.20494.3907	18 04 04.91	-29 11 37.9	19.98	0.66	1938.8	23.8	3.99	1.02	A	c	
114.20496.5206	18 04 09.01	-29 03 11.3	20.06	0.84	1748.4	107	15.8	0.68	A	c	
114.20621.2010	18 04 29.17	-29 22 22.9	18.83	0.73	2037.6	14.6	2.23	1.11	B	c	
114.20750.2236	18 04 51.50	-29 24 42.3	19.42	0.80	1183.0	5.15	3.01	0.68	B	c	
114.20751.4978	18 04 51.82	-29 22 40.3	20.06	0.87	1602.8	8.07	3.46	0.77	A	c	
115.22181.2973	18 08 01.71	-29 21 01.7	19.77	0.82	2719.8	10.4	1.90	0.77	C	e	
115.22435.1045	18 08 46.35	-29 44 13.8	18.64	0.78	2722.0	32.6	1.60	1.30	A	c	$R \neq B$

Table 3—Continued

field.tile.seq	$\alpha$ (2000)	$\delta$ (2000)	$V$	$V - R$	$t_0$	$\hat{t}$	$A_{max}$	$\frac{\chi^2}{n_{dof}}$	Gr.	Sel.	Notes
115.22442.1010	18 08 38.61	−29 17 23.6	18.52	0.77	2703.3	13.2	2.59	1.30	A	c	
115.22564.2355	18 09 00.22	−29 48 38.2	19.15	0.62	2428.8	9.68	1.64	1.29	C	e	$R \neq B$
115.22565.2060	18 09 02.87	−29 44 12.7	19.19	0.68	463.4	28.0	2.38	20	B	c	$R \neq B$
115.22698.3919	18 09 18.89	−29 32 58.8	19.89	0.44	1975.5	8.90	1.94	1.85	C	e	
115.22701.743	18 09 15.79	−29 19 49.1	18.16	0.77	1617.7	19.0	4.26	0.74	A	c	
115.22959.667	18 10 04.14	−29 31 03.5	17.85	0.76	1573.2	91.9	1.41	0.82	B	e	
116.23740.1193	18 11 40.72	−29 27 19.6	18.94	0.83	1636.0	16.2	7.96	0.31	A	c	
116.23864.503	18 12 07.28	−29 47 54.5	17.88	0.84	1971.2	41.3	2.57	1.42	A	c	
116.24255.4464	18 12 57.37	−29 45 11.0	20.10	0.61	2355.0	18.5	5.15	0.62	A	c	
116.24384.2597	18 13 14.33	−29 50 33.6	19.50	0.63	2401.1	28.3	1.93	0.89	B	c	
118.18009.35	17 58 25.53	−30 08 08.6	17.60	1.57	2808.6	55.5	2.58	3.98	A	e	$R \neq B$ var
118.18012.1863	17 58 14.82	−29 56 13.2	18.73	0.77	1969.3	29.8	1.64	0.66	B	c	
118.18014.320 <sup>†</sup>	17 58 25.30	−29 47 59.5	17.02	0.98	877.6	25.5	1.58	1.05	A	c	
118.18014.4514	17 58 29.84	−29 50 02.0	20.20	1.03	2794.5	42.7	1.68	1.15	C	e	
118.18015.1406	17 58 25.94	−29 44 47.7	18.75	1.03	878.0	9.78	1.41	0.69	B	e	
118.18018.2379	17 58 16.01	−29 32 10.9	19.09	0.84	1245.4	84.6	2.69	0.39	A	c	
118.18141.731 <sup>†</sup>	17 58 36.77	−30 02 19.3	17.93	1.07	884.1	9.77	12.6	0.65	B	cb	bin
118.18270.3615 <sup>s</sup>	17 59 04.77	−30 07 06.0	20.46	1.13	1893.4	9.91	2.52	0.87	B	c	
118.18271.738 <sup>†</sup>	17 58 52.46	−30 02 08.0	18.30	1.20	456.4	53.7	2.23	0.69	A	c	
118.18276.129	17 59 03.29	−29 42 59.8	17.16	0.53	530.7	14.5	4.06	0.88	A	c	
118.18278.3065	17 58 55.62	−29 34 24.7	20.21	0.88	594.5	21.1	1.79	1.28	A	c	
118.18402.495 <sup>†</sup>	17 59 13.85	−29 55 53.4	17.65	1.11	454.1	23.8	3.60	0.96	A	c	
118.18407.1167	17 59 16.32	−29 38 04.1	18.61	1.12	891.3	3.19	1.60	0.73	B	e	$R \neq B$
118.18529.538	17 59 35.34	−30 08 47.7	19.58	1.05	1952.0	97.4	17.0	1.44	A	c	
118.18531.1816	17 59 37.69	−30 00 52.7	19.27	0.85	1561.5	57.2	1.34	1.26	B	e	
118.18536.3276	17 59 34.61	−29 39 48.4	19.93	0.83	1060.5	142	2.93	0.66	C	c	
118.18660.3016	17 59 45.20	−30 05 18.6	19.88	0.96	1169.0	8.76	2.56	1.45	C	e	
118.18662.1151 <sup>t</sup>	17 59 46.51	−29 57 28.3	18.40	0.85	2622.7	15.1	3.18	0.76	A	c	
118.18662.2180	17 59 56.33	−29 56 38.0	19.65	1.00	1944.5	26.4	1.76	0.90	A	c	
118.18662.3919	17 59 57.17	−29 58 58.0	20.53	0.82	980.0	15.8	1.94	0.81	B	e	$R \neq B$
118.18668.3942	18 00 00.81	−29 32 40.0	20.51	1.04	954.5	12.4	2.04	1.52	B	e	
118.18669.3968	17 59 52.03	−29 31 14.4	20.71	1.04	1972.7	15.3	2.17	0.87	B	e	
118.18797.1397 <sup>†</sup>	18 00 06.94	−29 38 06.0	19.37	1.33	2013.1	126	8.35	1.07	A	c	
118.19182.891 <sup>†</sup>	18 01 09.75	−29 56 18.9	17.98	0.93	2367.0	13.6	6.28	1.2	A	c	
118.19184.1814	18 01 02.88	−29 48 40.2	18.70	0.73	2441.7	11.7	7.46	0.82	A	c	
118.19184.3770	18 00 58.13	−29 49 50.6	20.05	0.88	1601.1	12.2	3.75	0.89	A	c	
118.19184.939 <sup>†</sup>	18 01 10.23	−29 48 55.4	18.08	0.99	2692.8	74.4	2.14	1.13	A	c	
118.19311.1429	18 01 20.85	−30 00 08.6	20.49	1.06	599.7	6.81	2.11	1.05	B	e	
119.19441.2773	18 01 38.41	−30 02 02.6	19.58	0.71	1896.1	21.7	2.34	1.23	C	e	$R \neq B$
119.19442.370	18 01 51.03	−29 56 50.3	18.26	0.95	2776.0	49.7	1.31	10	A	a	
119.19444.2055	18 01 45.53	−29 49 46.9	19.24	0.79	1543.8	51.4	20.3	2.49	A	ab	bin
119.19568.3510	18 01 54.13	−30 12 17.4	19.75	0.79	2625.6	9.77	2.01	1.26	B	c	

Table 3—Continued

field.tile.seq	$\alpha$ (2000)	$\delta$ (2000)	$V$	$V - R$	$t_0$	$\hat{t}$	$A_{max}$	$\frac{\chi^2}{n_{dof}}$	Gr.	Sel.	Notes
119.19576.2024	18 02 04.77	−29 43 15.9	18.80	0.72	1371.0	40.0	2.27	1.29	A	c	$R \neq B$
119.19576.6481	18 01 56.62	−29 39 54.7	20.29	0.72	2697.0	6.92	4.32	0.87	B	e	$R \neq B$
119.19701.1513	18 02 11.79	−30 00 58.4	19.00	0.96	2700.6	26.2	1.53	2.15	B	c	
119.19704.5147	18 02 11.09	−29 51 21.1	20.15	0.80	1294.1	15.2	2.52	0.47	B	e	
119.19832.5483	18 02 44.85	−29 58 18.3	20.41	0.69	2366.0	36.1	2.14	0.64	B	c	
119.19834.46	18 02 37.08	−29 47 58.9	15.21	0.90	612.0	107	1.12	1.08	C	e	$R \neq B$
119.19835.4282	18 02 35.10	−29 47 18.7	19.72	0.71	1563.8	7.78	2.47	1.54	C	e	
119.19837.1072	18 02 37.51	−29 39 35.9	18.94	1.08	1185.8	2.47	5.43	1.38	A	c	
119.19959.4320	18 03 03.12	−30 09 56.5	19.93	0.71	488.9	56.5	2.36	1.17	C	e	bin
119.20088.2601	18 03 10.74	−30 15 33.5	20.24	0.79	538.8	7.14	3.09	1.10	B	e	
119.20091.1789	18 03 06.65	−30 02 37.5	19.44	0.67	2104.2	11.8	3.32	0.76	A	c	
119.20092.3109	18 03 10.93	−29 58 12.9	19.70	0.83	2690.4	17.7	2.23	0.74	A	c	
119.20219.2348	18 03 30.09	−30 09 55.9	19.39	0.88	2066.5	94.3	2.19	0.53	A	e	
119.20226.2119	18 03 35.79	−29 42 01.3	19.19	0.83	553.6	106	2.63	3.81	C	b	bin
119.20352.2589	18 03 58.67	−29 58 48.7	17.52	0.64	1987.4	24.9	1.76	1.57	A	c	bin $R \neq B$
119.20354.3615	18 03 42.72	−29 49 20.1	19.67	0.75	1213.6	24.6	1.43	1.2	B	e	
119.20356.407	18 03 54.14	−29 42 30.8	17.16	0.95	592.2	13.3	2.42	3.35	A	e	
119.20480.2914	18 04 16.37	−30 07 23.3	19.76	0.87	1938.1	52.3	1.89	1.08	A	c	
119.20610.5200	18 04 24.83	−30 05 58.9	20.41	0.71	531.9	50.1	2.59	0.79	A	e	
119.20611.6102	18 04 20.29	−30 02 22.1	20.66	0.68	2639.6	22.3	2.11	0.92	B	c	
119.20737.740	18 04 50.62	−30 16 34.2	18.56	1.01	2309.1	21.0	1.34	1.74	B	e	
119.20738.3418	18 04 37.24	−30 12 11.5	20.05	0.94	1229.9	26.8	28.3	0.45	A	c	
119.20741.4276 <sup>u</sup>	18 04 48.52	−30 01 15.7	19.78	0.84	564.3	15.4	1.90	0.74	C	e	
120.21010.1474	18 05 30.73	−29 26 15.1	17.86	0.77	1264.1	21.2	1.67	1.53	A	c	
120.21140.3398	18 05 33.87	−29 24 52.9	20.20	0.93	1648.2	14.9	1.70	0.99	C	a	
120.21263.1213	18 06 04.77	−29 52 38.1	18.89	0.89	1262.5	148	2.64	3.01	A	cb	bin
120.21392.1243	18 06 07.94	−29 59 26.1	18.95	0.97	2037.0	243	1.38	0.45	B	a	
120.21522.2448	18 06 35.36	−29 57 43.8	19.67	0.84	1173.7	10.6	5.65	1.11	B	e	
120.21523.2457	18 06 29.67	−29 53 06.3	19.63	0.82	1632.6	13.4	1.69	1.04	C	e	
120.21912.3560	18 07 37.03	−29 56 08.2	20.25	0.68	2474.3	71.0	5.83e+12	1.09	B	a	
120.21917.4650	18 07 26.44	−29 39 34.2	20.94	0.67	538.2	29.7	4.47	0.65	B	c	
120.22043.4380	18 07 50.84	−29 54 21.8	19.93	0.85	1980.5	57.9	2.41	0.92	B	c	bin
121.21903.1151 <sup>v</sup>	18 07 23.53	−30 32 55.4	19.30	0.81	470.9	31.5	5.06	0.91	A	c	
121.21909.1805	18 07 25.28	−30 09 39.0	19.41	0.74	1954.6	21.1	1.70	0.69	A	c	
121.21910.1940	18 07 33.59	−30 06 36.8	19.60	0.87	2031.1	7.35	1.86	1.50	A	e	
121.22032.133 <sup>†</sup>	18 07 46.89	−30 39 41.5	16.39	0.87	1287.3	19.5	1.58	2.51	A	c	
121.22033.917	18 07 56.49	−30 34 03.3	18.84	0.81	534.4	30.7	3.30	0.84	A	c	
121.22292.2289 <sup>w</sup>	18 08 23.17	−30 36 18.6	19.59	0.72	456.5	39.0	2.71	1.35	A	c	
121.22423.1032	18 08 49.98	−30 31 55.9	18.89	0.86	2718.8	432	3.52	2.60	A	c	
121.22425.177	18 08 51.10	−30 24 34.7	16.59	0.87	2766.7	7.45	3.07	0.89	A	a	
122.22816.2315	18 09 28.78	−30 22 40.7	19.93	0.94	1329.7	49.3	1.62	1.37	C	e	
122.23205.1241	18 10 40.17	−30 26 53.7	19.24	0.70	1308.2	9.06	2.24	0.70	A	c	

Table 3—Continued

field.tile.seq	$\alpha$ (2000)	$\delta$ (2000)	$V$	$V - R$	$t_0$	$\hat{t}$	$A_{max}$	$\frac{\chi^2}{n_{dof}}$	Gr.	Sel.	Notes
122.23855.1875	18 12 12.44	−30 26 19.2	19.32	0.58	561.5	10.1	1.65	0.67	B	e	
123.24378.2299	18 13 10.53	−30 11 43.1	20.00	0.72	481.2	17.1	1.64	0.71	B	c	
124.21377.353	18 06 23.60	−30 59 03.1	19.54	0.92	1677.4	34.9	1.79	1.04	A	c	
124.21503.1711	18 06 39.24	−31 15 19.4	19.64	0.89	2376.5	18.1	1.60	1.62	B	c	
124.22024.4124	18 07 51.91	−31 09 19.8	20.33	0.75	544.8	35.5	2.00e+3	0.89	A	e	
124.22155.295	18 08 11.48	−31 03 48.0	18.98	0.76	1299.9	42.2	1.43	1.06	A	e	
124.22157.151	18 08 14.74	−30 57 48.3	17.20	0.94	418.2	140	1.47e+4	1.43	A	e	
128.21145.1300	18 05 40.59	−29 05 59.7	18.89	0.87	1635.7	37.3	2.46	0.6	B	e	
128.21147.5157	18 05 36.49	−28 58 20.4	20.84	0.83	2653.2	14.4	4.12	0.80	B	e	
128.21407.2080 <sup>a,f</sup>	18 06 24.29	−28 55 46.7	19.18	0.78	2111.9	44.7	2.99	0.39	C	e	
128.21541.1133	18 06 42.40	−28 41 15.9	18.81	0.97	1749.7	53.8	5.81	10	A	c	
128.21666.982	18 06 57.62	−29 00 55.2	18.35	0.85	597.6	16.0	7.15	1.15	A	c	
128.21800.522	18 07 11.15	−28 46 58.9	18.26	0.97	1315.2	2.73	4.70	0.43	A	e	
128.21932.1362 <sup>a,g</sup>	18 07 20.58	−28 36 50.7	18.96	0.84	1285.4	72.8	1.71	1.48	B	c	
128.22057.2384	18 07 38.97	−28 57 11.8	19.17	0.60	1714.3	73.1	1.69	1.30	A	c	
130.28701.2042	18 23 11.74	−28 00 38.0	20.70	0.53	484.3	15.8	5.51	1.25	A	c	
130.28964.2444	18 23 50.50	−27 51 39.9	20.26	0.56	483.0	40.9	3.89	0.70	A	c	
131.29214.519 <sup>x</sup>	18 24 27.07	−28 31 37.3	18.21	0.57	1633.6	56.2	1.80	1.40	A	c	
132.30916.803	18 28 36.19	−27 42 47.7	19.14	0.60	958.5	22.1	1.70	0.86	A	c	
132.31306.841	18 29 33.12	−27 41 35.1	19.16	0.63	2739.8	147	2.60	1.33	A	c	
134.33390.299	18 34 25.64	−27 26 44.5	18.25	0.56	889.2	8.79	4.80	10	A	c	
136.27650.2370 <sup>y</sup>	18 21 01.78	−28 46 46.0	19.90	0.71	2044.7	115	4.91	1.24	A	c	
137.29210.2447	18 24 37.98	−28 43 43.8	20.16	0.66	874.2	61.9	1.52	1.11	B	c	
137.29214.59 <sup>x</sup>	18 24 27.05	−28 31 36.8	18.33	0.55	1634.6	52.5	1.81	1.16	A	c	$R \neq B$
137.29731.2320	18 25 46.34	−28 42 55.7	20.19	0.67	892.8	31.0	2.02	1.22	C	e	
137.29986.2769	18 26 29.74	−29 03 39.9	20.56	0.58	1620.0	64.8	7.36	1.02	A	c	
139.32203.2073	18 31 35.56	−28 34 04.8	20.27	0.57	2711.4	32.1	2.54	0.77	A	c	
142.27650.6057 <sup>y</sup>	18 21 01.83	−28 46 45.0	19.87	0.68	2044.4	109	4.86	0.99	A	c	
142.27776.3952	18 21 03.28	−29 01 06.0	20.91	0.73	2351.6	66.7	4.43	0.6	B	c	
144.32453.1528	18 32 14.17	−29 12 07.0	20.43	0.73	940.7	7.83	3.25	1.56	C	e	
148.26586.2310	18 18 24.33	−30 23 37.1	19.72	0.59	2312.1	32.6	3.56	1.31	A	e	$R \neq B$
148.26590.3689	18 18 33.14	−30 04 48.5	21.24	1.18	1488.9	421	114	20	C	e	
149.27233.2244	18 19 50.87	−30 34 50.4	20.71	0.62	497.6	39.0	2.59	0.64	B	e	
149.27237.3033	18 19 51.90	−30 16 00.0	20.87	0.72	850.4	24.3	2.78	0.91	B	e	
150.28409.2370	18 22 45.01	−30 08 46.0	20.48	0.38	2500.6	446	1.91	1.21	C	e	
151.31133.1607	18 28 59.51	−30 31 54.5	19.88	0.46	883.8	11.9	1.61	1.63	B	e	
152.26320.2643	18 17 52.02	−30 45 06.1	20.17	0.46	921.7	54.7	2.11	1.04	B	e	
152.26964.3183	18 19 16.03	−31 10 47.0	20.41	0.64	2697.3	22.1	1.75	0.85	B	c	
153.27488.3450	18 20 36.33	−30 54 01.5	20.55	0.38	1265.4	50.8	5.89	1.42	B	e	$R \neq B$
153.28787.720 <sup>z</sup>	18 23 34.30	−30 57 56.0	18.03	0.63	915.0	167	2.50	0.68	A	c	
154.28787.2812 <sup>z</sup>	18 23 34.31	−30 57 55.9	18.52	0.59	915.1	169	2.53	0.90	A	c	
154.29041.2113	18 24 06.12	−31 20 33.8	20.31	0.53	1587.3	46.9	2.01	1.08	A	c	

Table 3—Continued

field.tile.seq	$\alpha$ (2000)	$\delta$ (2000)	V	$V - R$	$t_0$	$\hat{t}$	$A_{max}$	$\frac{\chi^2}{n_{dof}}$	Gr.	Sel.	Notes
154.29175.2554	18 24 36.47	−31 05 27.1	20.85	0.61	1591.1	55.1	4.15	0.74	B	c	
155.26043.1938	18 17 22.14	−31 54 54.0	19.67	0.44	1979.4	8.52	1.58	0.81	C	e	
156.27606.899	18 20 54.08	−31 41 12.6	19.12	0.50	1615.3	15.5	1.89	0.65	A	c	
158.26536.1361	18 18 02.24	−25 01 37.4	19.30	0.82	1286.6	28.1	2.07	1.05	B	e	
158.26665.3141	18 18 27.21	−25 05 56.5	19.96	0.66	2007.6	11.5	1.58	0.78	C	e	$R \neq B$
158.26802.1155	18 18 43.16	−24 37 43.7	19.83	0.84	2018.0	47.7	1.97	0.97	B	c	
158.27052.2802	18 19 24.84	−25 18 10.2	19.78	0.67	2085.5	142	4.94e+5	0.91	A	e	
158.27444.129 <sup>†</sup>	18 20 10.24	−25 08 26.0	16.97	0.77	2376.4	41.7	2.31	1.80	A	c	
159.25486.1627	18 15 42.82	−25 41 03.2	19.49	0.86	2010.2	68.3	1.83	0.84	C	c	
159.25615.941	18 15 54.71	−25 43 59.5	18.73	0.77	2681.1	58.8	2.62	0.44	A	c	$R \neq B$
159.25748.2254	18 16 16.98	−25 32 25.7	19.69	0.80	2364.9	39.1	2.35	0.85	B	c	
159.25872.1610	18 16 33.13	−25 57 52.6	19.23	0.55	1284.1	15.8	1.95	0.88	B	c	
159.26132.3182	18 17 14.80	−25 55 58.0	20.90	0.79	1277.0	26.6	5.32	1.7	B	e	
159.26525.1401	18 18 07.98	−25 46 46.9	21.29	0.71	507.4	72.7	9.90	1.12	A	c	
160.27701.3570	18 20 49.55	−25 20 14.0	20.05	0.66	1650.5	27.4	1.75	1.15	B	e	
161.24182.1566	18 12 44.08	−25 57 17.6	19.97	1.07	1952.8	110	3.92	1.26	A	c	
161.24568.876	18 13 29.30	−26 13 58.1	18.51	0.69	1219.1	21.1	2.27	1.08	A	c	
161.24695.1323	18 14 00.99	−26 27 21.6	18.62	0.74	1668.8	57.9	1.69	0.68	A	c	
161.24696.1161	18 13 51.87	−26 20 42.1	18.83	0.84	559.2	36.2	2.28	0.67	C	e	
161.24827.4269	18 14 13.00	−26 16 49.6	20.58	0.83	1553.0	23.3	2.35	0.79	B	c	
161.24956.2466	18 14 31.72	−26 20 17.3	19.77	0.92	2307.4	98.7	1.71	0.75	A	c	
162.25212.3830	18 14 59.66	−26 36 48.1	20.18	0.77	587.4	43.8	2.12	0.70	B	c	
162.25865.442 <sup>†</sup>	18 16 30.60	−26 26 58.3	17.54	0.90	1225.3	60.9	1.58	1.32	A	c	
162.25868.405 <sup>†</sup>	18 16 45.98	−26 11 43.1	17.33	0.83	1222.8	30.8	2.77	1.39	A	c	
162.25869.432 <sup>aa</sup>	18 16 44.34	−26 09 25.7	17.52	0.71	522.0	26.6	2.26	2.08	A	c	bin
163.27297.2111	18 19 52.42	−26 18 05.4	20.25	0.68	505.1	23.9	2.50	1.81	C	e	$R \neq B$
163.27684.1669	18 20 48.38	−26 31 06.2	19.63	0.77	1600.1	12.9	1.65	0.82	B	c	
166.30682.3768	18 27 46.30	−25 57 08.8	21.19	0.82	497.6	35.2	3.16	0.77	B	e	
167.23910.3170	18 11 55.15	−26 46 32.7	20.03	0.86	1607.9	65.5	1.79	1.38	B	c	
167.24169.3673	18 12 45.02	−26 50 53.4	20.16	0.74	564.9	45.5	2.20	0.74	C	e	
167.24173.2623	18 12 44.90	−26 34 50.3	19.62	0.73	1722.1	93.8	1.10e+3	0.97	B	e	
167.24564.5066	18 13 32.15	−26 31 10.3	20.36	0.87	484.1	32.8	3.03	0.81	A	c	
167.24815.4558	18 14 09.36	−27 04 57.7	20.20	0.73	1954.8	8.05	2.89	0.87	B	e	$R \neq B$
167.24815.4984	18 14 06.96	−27 05 38.0	20.59	0.90	1296.9	38.9	2.46	0.63	B	e	
168.25079.1100	18 14 56.37	−26 51 09.9	17.89	1.65	550.8	47.8	1.52	1.35	B	e	
168.25853.1778	18 16 30.98	−27 14 18.7	18.83	0.63	501.5	43.8	1.59	0.69	B	c	
168.25985.4014	18 17 01.65	−27 05 45.0	20.63	0.67	1476.1	360	18.1	1.76	B	e	
172.31579.2624	18 30 07.75	−26 48 20.5	20.37	0.69	2736.5	128	2.31	1.33	B	c	
172.32358.313	18 31 53.24	−26 51 42.6	18.15	0.58	2700.9	42.0	1.63	0.92	A	c	
174.29360.352	18 24 42.09	−27 25 41.6	17.59	0.66	2735.7	75.5	17.7	1.32	A	c	
175.31446.1290	18 29 34.21	−27 03 14.2	20.96	0.82	845.1	23.4	2.17	0.76	C	c	
176.18693.267	17 59 46.63	−27 53 51.4	17.72	1.43	2344.5	6.36	1.29e+8	2.18	A	e	

Table 3—Continued

field.tile.seq	$\alpha$ (2000)	$\delta$ (2000)	$V$	$V - R$	$t_0$	$\hat{t}$	$A_{max}$	$\frac{\chi^2}{n_{dof}}$	Gr.	Sel.	Notes
176.18826.909 <sup>†</sup>	18 00 15.45	-27 42 47.8	18.78	1.21	2364.7	24.3	1.77	1.17	A	c	
176.18827.1911	18 00 11.98	-27 36 10.6	19.59	0.96	2346.3	20.3	2.27	1.06	A	c	
176.18954.6538	18 00 20.85	-27 48 31.2	21.39	0.93	2657.1	94.7	3.74	1.06	B	c	
176.19214.2902	18 01 01.99	-27 51 26.5	20.83	1.04	1264.6	48.1	2.91	0.71	B	c	
176.19214.5296	18 01 11.11	-27 49 22.2	20.43	0.97	1907.7	14.7	2.44	0.98	A	e	
176.19219.978	18 01 04.41	-27 30 41.4	18.77	1.30	1228.9	56.7	4.71	4.40	A	b	bin
176.19343.5828	18 01 27.84	-27 52 21.0	20.13	0.72	2665.1	18.0	1.81	0.73	C	a	
176.19602.1226	18 01 59.22	-27 56 34.4	20.20	0.90	2754.2	62.4	2.23	1.27	B	c	
176.19735.2709	18 02 20.27	-27 45 53.4	19.59	0.91	2025.5	12.0	1.72	1.12	B	c	
176.19997.3338	18 02 48.51	-27 38 51.8	20.70	1.05	2790.0	75.6	1.11e+4	1.23	B	a	
177.25109.1274	18 14 54.37	-24 49 34.9	21.07	1.05	1261.0	55.5	4.89	0.58	B	c	
177.25111.120	18 14 52.70	-24 41 07.9	17.21	1.20	1566.9	25.9	7.64	2.20	A	c	
177.25756.2480	18 16 24.87	-25 03 26.5	20.41	1.01	2025.2	18.5	1.65	0.94	B	e	
178.23136.5133	18 10 10.18	-26 21 03.6	20.32	0.74	1915.9	157	5.92	0.40	A	e	
178.23273.6023	18 10 38.12	-25 53 15.3	20.59	0.95	2362.9	11.8	57.0	0.87	C	a	
178.23398.4814	18 10 59.48	-26 13 16.5	20.51	0.94	2420.4	37.1	2.90	0.74	A	c	
178.23531.931 <sup>†</sup>	18 11 17.41	-25 59 51.4	18.72	1.11	1590.3	13.7	2.18	1.08	A	c	
178.23660.2137	18 11 23.70	-26 04 57.0	20.58	1.02	1191.4	101	3.63	0.82	B	c	
179.21577.1740	18 06 31.70	-26 16 01.6	19.79	0.99	2327.8	23.3	9.32	7.51	A	b	bin
179.21578.2080	18 06 32.82	-26 15 13.6	20.80	1.41	2382.4	63.0	8.16	1.24	A	c	
179.21584.3189	18 06 28.52	-25 49 02.1	21.08	1.26	2690.3	34.9	1.52	0.75	B	a	
179.21844.84	18 07 08.43	-25 49 20.7	16.98	1.36	1970.2	80.6	1.68	1.86	A	c	
179.21971.6468	18 07 28.27	-25 59 59.7	21.53	1.24	2369.2	34.8	2.37	0.80	B	e	
179.21971.936	18 07 22.06	-25 59 44.7	19.00	1.19	2618.6	20.9	2.95	0.91	A	a	
179.22226.151	18 07 59.13	-26 22 46.8	17.49	1.30	2581.0	70.9	1.11e+16	1.02	B	a	
179.22486.3353	18 08 34.24	-26 21 13.6	20.08	0.91	1615.0	20.6	3.37	0.94	A	c	
179.22616.2234	18 09 08.05	-26 20 34.3	19.77	1.06	2321.9	13.9	27.7	1.44	C	e	
179.22619.3190	18 08 58.42	-26 08 07.6	21.06	1.33	1623.5	174	4.27	0.79	B	c	bin
180.22240.202 <sup>†</sup>	18 07 57.82	-25 24 48.1	18.98	1.44	1286.9	311	3.42	1.15	A	c	
180.22242.2664	18 08 09.34	-25 15 56.7	20.15	1.01	2426.9	9.88	1.70	0.86	B	e	
180.22633.2883	18 08 58.65	-25 14 22.3	20.56	1.06	2760.5	25.7	3.71	0.82	A	c	
180.22759.707	18 09 17.80	-25 29 03.7	19.21	1.15	2832.0	71.8	2.14	1.98	A	a	
180.22767.1452	18 09 15.50	-24 58 14.9	20.33	1.30	1957.9	22.2	7.92	1.40	A	c	
180.23412.3949	18 10 53.70	-25 17 28.0	21.18	1.14	2358.8	19.2	2.11	0.89	B	c	
301.45441.747	18 31 36.15	-13 31 37.4	21.56	1.37	2682.9	45.4	5.23	1.07	C	c	
301.45445.840	18 31 38.13	-13 16 01.1	19.32	1.00	1895.4	197	1.81	0.92	B	a	bin
301.46110.1056	18 32 43.60	-13 44 19.0	19.81	1.15	1951.2	98.5	2.10	0.87	A	c	
301.46285.1166	18 33 09.38	-13 16 54.1	21.20	1.20	2661.8	279	3.69	0.76	C	c	
301.46613.3271	18 33 38.09	-13 50 23.9	20.99	1.06	2079.3	112	2.68	0.99	B	c	
301.46616.2156	18 33 36.01	-13 35 09.1	20.18	0.94	1962.7	41.3	2.55	0.98	A	c	
302.44927.2559	18 30 41.95	-14 14 08.1	19.52	0.97	1993.3	86.2	1.41	1.29	B	e	
302.44928.3523	18 30 49.42	-14 10 52.9	21.41	1.07	2770.3	86.7	25.4	1.12	A	c	bin

Table 3—Continued

field.tile.seq	$\alpha$ (2000)	$\delta$ (2000)	$V$	$V - R$	$t_0$	$\hat{t}$	$A_{max}$	$\frac{\chi^2}{n_{dof}}$	Gr.	Sel.	Notes
302.45258.1038	18 31 20.04	-14 34 07.9	19.05	0.81	1605.1	146	1.99	0.94	A	c	
304.35391.650	18 15 08.27	-22 45 05.1	20.04	0.90	1252.8	10.9	1.58	0.78	C	e	
304.35564.26	18 15 11.46	-22 22 59.1	17.64	1.78	1705.4	25.4	2.11	1.97	A	c	
304.35730.425	18 15 35.67	-22 32 11.2	19.43	1.41	2686.1	81.9	2.42	0.87	A	c	
304.35899.3004	18 15 54.97	-22 27 33.5	21.17	1.12	2632.6	38.5	3.42	0.67	B	e	
304.36403.2137	18 16 38.95	-22 28 52.8	21.12	1.05	1244.5	57.6	2.25	0.99	B	c	
304.36904.698	18 17 24.55	-22 41 57.2	19.94	1.04	1750.6	208	2.11	0.94	B	c	
305.35237.685	18 14 43.51	-21 48 10.6	19.65	1.11	2655.4	260	1.47	1.66	C	e	
305.35738.35	18 15 36.08	-22 01 54.7	17.43	1.80	1285.9	36.2	4.52	2.95	A	c	
305.36746.2411	18 17 16.16	-22 01 18.3	20.75	1.17	2375.6	40.7	69.0	0.86	A	c	
306.35894.1371	18 15 53.15	-22 47 22.9	20.64	1.17	1192.5	184	2.51	0.76	A	e	
306.36223.3023	18 16 32.59	-23 17 26.8	20.29	0.86	1921.5	11.4	2.27	1.35	B	c	
307.35374.3058	18 15 02.51	-23 52 41.5	20.95	1.14	2740.4	50.7	2.67	0.85	B	c	
307.35709.1490	18 15 37.63	-23 55 11.1	19.68	0.93	1557.6	15.3	2.33	0.96	B	e	
307.36378.482	18 16 35.35	-24 09 12.5	19.61	1.22	1267.3	32.8	1.58	0.82	B	c	
307.36884.258 <sup>ab</sup>	18 17 28.63	-23 59 45.9	17.69	1.10	1315.4	30.8	2.32	0.85	A	c	
308.38259.1981	18 19 43.15	-21 57 45.4	20.15	0.76	2388.3	8.30	1.54	2.37	C	e	
308.38595.1020	18 20 30.03	-21 57 04.3	19.81	1.01	2769.4	58.0	14.2	1.2	A	c	
309.38081.3420	18 19 30.55	-22 37 56.0	21.12	1.01	1712.1	68.4	5.48	0.69	B	c	
310.37067.3803	18 17 50.51	-23 02 22.8	21.12	0.96	1605.6	10.8	2.20	1.34	C	e	
310.37233.3924	18 18 06.37	-23 10 06.5	20.77	0.92	1230.4	11.8	4.69	0.74	B	e	
310.37235.3685	18 18 04.38	-23 02 11.1	21.15	1.09	2056.8	70.0	2.98	0.87	A	c	
310.37398.2274	18 18 19.82	-23 19 08.9	21.00	0.85	1283.1	118	2.20	0.68	B	c	
310.37400.1067	18 18 19.85	-23 14 45.3	19.43	0.98	2663.3	83.7	4.74	0.69	A	c	
310.37407.336	18 18 28.16	-22 45 50.9	18.75	1.02	2802.6	182	1.52	1.86	C	c	bin
310.38237.1062	18 19 52.32	-23 25 35.7	18.94	0.81	1311.7	11.9	1.57	0.81	C	e	$R \neq B$
310.38242.570	18 19 40.58	-23 04 44.2	20.00	0.94	1304.2	11.3	1.55	2.71	C	e	$R \neq B$
310.38407.3684	18 19 56.45	-23 18 41.4	20.64	0.80	2726.0	639	1.71	1.30	D	c	
310.38573.911	18 20 24.90	-23 25 17.5	19.34	0.87	1222.5	127	1.95	0.85	A	c	
311.36884.287 <sup>ab</sup>	18 17 28.62	-23 59 47.0	17.55	0.93	1315.4	30.9	2.42	0.65	A	c	
311.36890.444	18 17 39.60	-23 36 07.4	18.67	1.09	2813.1	200	4.38	1.49	A	c	
311.37050.344	18 17 45.38	-24 09 04.0	17.93	0.80	1295.2	27.4	1.40	1.09	A	e	
311.37223.967	18 18 10.73	-23 47 16.5	20.99	1.09	1600.6	21.8	3.76	0.56	A	c	
311.37727.1742	18 18 59.74	-23 49 26.7	20.10	0.95	1577.7	99.5	3.05	1.25	B	c	bin
311.37893.6302	18 19 20.38	-23 55 36.9	21.47	0.77	2705.9	71.5	11.5	0.76	A	c	
311.38229.2494	18 19 43.81	-23 58 55.4	19.52	0.66	2689.3	5.79	1.67	1.82	C	e	
311.38394.386	18 20 04.48	-24 08 11.1	19.65	0.76	1268.3	31.1	3.14	1.49	A	c	bin
311.38567.3476	18 20 19.31	-23 49 41.5	20.32	0.79	2028.1	7.20	1.80	1.19	C	e	
401.47870.1026	17 56 22.00	-28 14 32.3	18.75	1.23	2433.3	51.7	1.49	1.33	B	e	
401.47990.2762	17 56 51.83	-28 14 47.7	20.28	1.32	1714.1	118	2.18	0.78	B	c	
401.47991.1840 <sup>†</sup>	17 57 07.51	-28 13 44.2	19.48	1.39	1953.0	44.7	1.92	0.61	A	c	
401.47994.1182 <sup>†</sup>	17 57 07.82	-28 00 27.9	19.68	1.55	2362.7	60.6	3.68	1.05	A	c	

Table 3—Continued

field.tile.seq	$\alpha$ (2000)	$\delta$ (2000)	$V$	$V - R$	$t_0$	$\hat{t}$	$A_{max}$	$\frac{\chi^2}{n_{dof}}$	Gr.	Sel.	Notes
401.48047.3195	17 57 14.57	−28 29 23.9	20.05	1.09	2272.9	46.9	2.19	0.41	B	c	
401.48049.670	17 57 13.63	−28 19 12.3	18.34	1.14	1587.0	25.1	1.34	1.74	C	e	
401.48052.861 <sup>†</sup>	17 57 23.81	−28 10 24.6	18.77	1.32	2291.5	72.0	2.65	0.69	B	c	
401.48114.174	17 57 42.91	−28 01 02.6	18.72	1.96	2624.0	51.9	6.79	0.66	A	c	
401.48167.1934 <sup>†</sup>	17 57 57.40	−28 27 09.6	18.44	1.23	2179.0	125	2.53	0.89	C	c	
401.48167.2536	17 58 00.72	−28 27 24.3	19.59	1.32	2682.2	14.1	1.40	1.07	B	e	
401.48229.760 <sup>†</sup>	17 58 13.42	−28 20 32.2	18.07	1.15	2694.5	20.1	1.82	1.18	A	c	bin $R \neq B$
401.48230.2825	17 58 13.75	−28 17 16.2	20.07	1.00	1698.3	9.43	6.43	0.46	A	c	
401.48406.2341	17 59 01.59	−28 31 28.1	20.09	1.09	2340.3	7.64	2.83	1.15	B	e	
401.48408.649 <sup>†</sup>	17 59 08.99	−28 24 54.7	17.72	1.22	2325.4	74.6	3.07	1.30	B	cb	bin
401.48410.1407	17 58 58.85	−28 16 30.2	18.83	1.20	2022.4	6.70	1.81	1.54	B	e	
401.48467.4621	17 59 16.98	−28 29 42.0	20.12	0.93	2339.8	45.2	2.57	1.11	A	c	
401.48469.789 <sup>†</sup>	17 59 22.27	−28 20 21.9	18.22	1.18	1554.8	5.67	5.96	0.42	B	c	
402.47619.1009	17 55 13.59	−28 58 33.6	20.23	1.09	1605.1	31.2	3.25	2.4	B	c	bin
402.47623.80	17 55 15.07	−28 43 23.6	18.62	2.42	2139.5	341	1.59	5.36	D	c	var
402.47678.1353	17 55 21.18	−29 04 12.6	18.89	1.24	2470.2	21.9	1.65	0.95	B	e	
402.47678.1666 <sup>†</sup>	17 55 22.60	−29 04 12.9	19.21	1.33	2393.1	13.6	2.48	0.88	A	c	
402.47681.2971	17 55 28.72	−28 50 43.5	19.96	1.22	1731.8	29.6	3.32	0.85	B	e	
402.47682.912	17 55 34.50	−28 48 26.8	18.79	0.88	1550.4	243	2.77	1.27	A	c	
402.47736.2869	17 55 45.00	−29 13 59.1	19.58	1.07	2647.2	58.0	2.45	0.54	B	e	
402.47737.1590 <sup>†</sup>	17 55 41.50	−29 09 00.6	18.49	1.05	1552.3	5.47	2.79	1.03	B	c	
402.47742.3318 <sup>†</sup>	17 55 42.88	−28 49 17.6	20.21	1.63	1377.1	50.1	8.64	1.21	A	c	
402.47745.3587	17 55 52.82	−28 36 43.7	21.10	1.27	2763.1	28.3	2.52	0.93	C	c	
402.47796.1893 <sup>†</sup>	17 56 10.91	−29 10 44.2	19.51	1.34	1678.7	19.3	22.5	1.47	B	c	
402.47797.1914	17 56 09.36	−29 08 30.2	19.70	1.43	2725.3	18.8	1.49	0.92	B	e	$R \neq B$
402.47798.1259 <sup>†</sup>	17 56 11.12	−29 06 13.9	19.75	1.40	1583.7	47.6	4.94	1.38	A	c	
402.47798.2435	17 56 04.72	−29 05 20.8	20.07	1.13	1908.2	68.3	2.15	0.29	C	e	
402.47799.1736 <sup>†</sup>	17 56 07.24	−28 58 32.6	19.59	1.29	2410.0	115	2.26	0.47	A	c	
402.47804.4101	17 56 02.99	−28 38 47.9	20.43	1.26	2657.6	12.6	2.25	1.59	C	c	$R \neq B$
402.47805.1858	17 55 56.31	−28 37 09.0	19.18	1.09	1924.7	7.40	1.71	1.04	C	e	
402.47856.561 <sup>†</sup>	17 56 25.05	−29 12 56.5	18.82	1.39	1566.6	12.3	2.14	1.63	B	c	
402.47862.1576 <sup>†</sup>	17 56 20.69	−28 47 42.0	19.48	1.31	2028.5	54.3	7.52	6.13	A	cb	bin
402.47862.3234	17 56 19.14	−28 47 20.3	20.50	1.21	1649.0	50.0	2.88	0.90	B	c	
402.47863.110	17 56 18.16	−28 46 05.0	16.64	1.18	2312.4	13.6	1.57	0.92	B	ab	bin
402.47978.4996	17 57 07.44	−29 05 28.7	20.86	0.97	2039.1	5.59	3.33	0.83	B	e	
402.48103.1719	17 57 32.81	−28 42 45.4	19.66	1.11	2395.9	425	4.37	1.25	A	c	
402.48156.2413	17 57 46.25	−29 12 04.6	20.17	1.02	1604.3	42.8	2.41	0.95	B	c	
402.48156.4509	17 57 51.08	−29 13 55.4	19.84	1.04	1327.0	28.9	2.21	0.83	A	c	
402.48158.1296 <sup>†</sup>	17 57 47.57	−29 03 54.3	18.69	1.12	2325.7	15.9	3.94	0.98	A	c	
402.48219.2582	17 58 15.37	−29 01 38.2	19.39	1.05	2257.9	12.9	3.94e+12	1.12	A	c	
402.48219.5086	17 58 05.42	−29 02 27.4	20.54	1.23	1538.9	17.9	2.17	0.85	B	c	
402.48279.1043	17 58 22.79	−28 59 54.5	19.63	1.05	1990.5	33.0	3.25	0.62	A	c	

Table 3—Continued

field.tile.seq	$\alpha$ (2000)	$\delta$ (2000)	$V$	$V - R$	$t_0$	$\hat{t}$	$A_{max}$	$\frac{\chi^2}{n_{dof}}$	Gr.	Sel.	Notes
402.48280.502 <sup>ac†</sup>	17 58 25.07	-28 57 46.3	18.16	1.18	1342.5	25.5	2.08	1.14	A	c	
403.47427.353	17 54 22.62	-29 49 57.4	19.01	0.94	2688.5	18.3	2.00	0.91	B	c	
403.47491.770 <sup>†</sup>	17 54 38.66	-29 33 12.8	17.95	1.29	2633.9	48.5	2.43	0.99	A	c	
403.47546.2003	17 54 43.89	-29 51 19.5	18.76	1.10	2436.3	65.8	1.48	0.68	B	e	
403.47548.1799	17 54 46.89	-29 44 17.1	18.87	1.09	2757.3	7.05	2.46	1.14	B	e	
403.47550.807 <sup>†</sup>	17 55 00.07	-29 35 03.8	17.95	1.21	2774.3	11.6	3.60	0.87	A	c	
403.47554.630	17 54 49.36	-29 20 24.8	18.14	1.30	2291.7	31.1	1.45	1.36	B	e	
403.47605.5112	17 55 11.84	-29 55 25.2	20.39	0.93	1606.4	3.96	2.93	0.51	B	c	
403.47610.576 <sup>†</sup>	17 55 17.07	-29 37 40.7	17.52	1.11	2657.9	9.59	4.75	2.56	A	c	$R \neq B$
403.47669.1859	17 55 36.42	-29 42 13.9	18.55	1.22	2078.3	26.5	1.47	1.40	B	e	
403.47670.5074	17 55 25.15	-29 34 50.2	20.25	0.86	1887.7	51.2	6.07	1.15	B	e	
403.47671.57	17 55 28.68	-29 33 41.7	16.07	1.33	2058.8	37.0	5.68	1.26	A	c	
403.47728.5938	17 55 55.62	-29 45 17.7	20.78	1.08	2338.4	13.1	3.90	1.09	B	c	
403.47785.3267	17 56 10.68	-29 56 57.2	19.95	1.06	1330.4	12.2	2.37	0.69	B	e	
403.47788.5281	17 56 06.47	-29 46 16.5	20.96	0.95	1667.8	36.4	16.8	0.70	B	e	
403.47790.3199	17 56 12.84	-29 37 35.1	21.19	1.05	2019.5	28.8	9.08	0.56	A	c	
403.47793.1349	17 56 10.97	-29 26 15.8	19.95	1.07	2082.2	18.0	1.79	0.66	B	e	
403.47793.2961 <sup>ad</sup>	17 55 57.99	-29 26 12.2	18.85	1.44	1688.6	24.1	2.50	1.2	B	b	bin
403.47845.495 <sup>†</sup>	17 56 22.79	-29 55 16.4	18.22	1.24	1945.8	15.0	2.03	0.88	A	c	
403.47846.2778	17 56 14.29	-29 50 58.2	20.21	1.13	2429.0	11.6	2.07	1.09	C	a	
403.47848.35	17 56 30.71	-29 46 29.6	16.06	1.58	2335.2	18.2	1.91	5.10	A	e	var
403.47849.756	17 56 25.18	-29 40 31.2	15.85	1.32	2732.7	293	4.30	6.37	A	e	
403.47907.3004	17 56 48.81	-29 49 31.3	20.20	1.02	1716.5	15.9	5.42	0.84	B	c	
403.47912.376	17 56 36.14	-29 29 19.2	18.54	1.80	2545.8	179	1.68	1.39	C	e	

Note. — The dagger symbol ( $\dagger$ ) denotes clump giants. Letter superscripts denote the same event found in multiple objects, the other event in the pair may be present in Table 4. The grades (column 10) are on an A-F scale, and the selection methods (column 11) are “c” for our clump-like selection criteria, “e” for events found by eye, “a” for events found via the alert system, and “b” for events from the binary paper.

Table 4. Parameters for Non-microlensing Events

field.tile.seq	$\alpha$ (2000)	$\delta$ (2000)	$V$	$V - R$	$t_0$	$\hat{t}$	$A_{max}$	$\frac{\chi^2}{n_{dof}}$	Gr.	Sel.	Notes
101.20650.3427 <sup>a</sup>	18 04 20.25	-27 24 47.3	19.61	0.77	1971.2	12.7	2.75	0.6	B	e	
101.21042.1247 <sup>c</sup>	18 05 28.07	-27 16 21.3	17.92	0.59	2806.9	19.3	1.64	0.55	B	e	
101.21174.3112 <sup>d</sup>	18 05 38.77	-27 08 28.4	19.59	0.89	1908.5	9.89	1.83	0.78	C	e	$R \neq B$
102.22851.5108 <sup>e</sup>	18 09 30.47	-28 00 49.2	20.48	0.80	1307.6	15.9	2.25	0.84	C	e	
104.19991.1951	18 03 01.33	-28 01 45.1	19.34	0.83	1739.0	54.4	2.96	1.80	C	c	cv
104.21421.273 <sup>ae</sup>	18 06 08.61	-28 00 24.7	18.61	0.70	2641.0	6.57	8.30	1.15	B	e	
105.21291.7441	18 05 53.59	-28 03 29.8	18.59	0.79	1603.1	8.11	2.53	3.46	C	e	cv
108.18943.3528 <sup>m</sup>	18 00 21.74	-28 32 01.1	19.34	0.84	2271.8	20.0	4.68e+10	0.54	C	e	
108.19341.2253 <sup>n</sup>	18 01 28.51	-28 02 15.4	19.90	0.89	2356.0	26.1	3.95	0.69	B	e	
109.19986.3305 <sup>p</sup>	18 03 01.12	-28 21 09.5	19.33	0.70	1258.6	19.9	2.19	0.72	B	e	
109.20370.5051 <sup>q</sup>	18 03 58.70	-28 47 40.3	20.16	0.81	2787.7	10.2	7.29	0.82	B	e	
113.18676.5195	18 00 01.25	-29 02 06.4	19.86	0.73	2255.4	12.5	2.03	2.25	C	e	cv
113.18810.4409 <sup>r</sup>	18 00 06.69	-28 44 00.3	20.04	0.82	2333.2	25.0	2.32	0.82	B	e	
114.19842.2283	18 02 40.21	-29 19 20.1	19.67	1.11	1721.6	12.1	1.74	1.7	C	a	cv
115.22695.3361	18 09 13.79	-29 47 36.4	19.77	0.66	2657.3	21.7	2.15	2.19	C	e	cv $R \neq B$
118.18270.4540 <sup>s</sup>	17 59 04.60	-30 07 06.7	20.53	1.02	1894.2	6.11	2.04	0.96	B	e	
118.18662.2288 <sup>t</sup>	17 59 46.56	-29 57 30.1	19.65	0.99	2623.5	14.0	2.61	0.53	C	e	
119.19707.2379	18 02 25.95	-29 39 40.4	19.84	0.80	2770.3	20.5	1.53	1.52	D	c	cv
119.20742.2884 <sup>u</sup>	18 04 48.74	-29 58 35.5	19.29	0.83	564.9	9.90	1.69	0.78	C	e	
121.21903.3479 <sup>v</sup>	18 07 23.50	-30 32 56.6	20.27	0.84	467.7	37.4	3.06	0.38	B	e	
121.22292.3358 <sup>w</sup>	18 08 23.00	-30 36 18.1	19.88	0.68	457.6	38.0	2.11	0.94	A	c	
125.23850.4190	18 11 58.88	-30 43 54.0	20.71	0.74	2724.1	18.9	2.64	0.77	C	a	cv
128.21407.1674 <sup>af</sup>	18 06 24.32	-28 55 47.9	18.91	0.92	2106.5	27.9	2.45	0.67	B	e	$R \neq B$
128.21926.3361	18 07 33.92	-29 00 36.5	19.52	0.67	552.2	15.2	2.00	1.24	C	e	cv $R \neq B$
128.21932.2196 <sup>ag</sup>	18 07 20.51	-28 36 51.9	19.66	1.07	1283.8	69.1	1.45	0.79	C	e	
145.34015.1280	18 35 55.58	-29 04 44.2	24.41	0.37	854.9	168	33.2	1.37	C	c	cv
153.28398.2677	18 22 35.67	-30 54 35.3	22.95	-0.06	858.7	134	10.1	0.67	D	c	cv $R \neq B$
162.25869.1615 <sup>aa</sup>	18 16 44.38	-26 09 27.2	20.10	0.74	523.6	72.8	4.52	0.40	A	c	
173.33002.479	18 33 17.45	-27 16 09.2	19.54	0.50	953.4	37.2	1.91	4.91	B	e	cv $R \neq B$
178.23266.2918	18 10 35.18	-26 23 40.4	19.91	0.94	1323.5	6.99	7.00e+5	1.14	C	e	cv
178.24048.3166	18 12 20.91	-26 14 03.0	20.54	0.73	2035.5	11.4	3.01	2.05	B	e	cv $R \neq B$
306.36059.752	18 16 05.96	-23 02 38.9	25.20	-0.39	1265.1	536	130	5.90	D	c	cv $R \neq B$
311.37730.4143	18 18 50.30	-23 36 14.9	21.89	0.76	1271.6	26.8	5.64	1.92	C	e	cv $R \neq B$
402.48280.894 <sup>ac</sup>	17 58 25.01	-28 57 44.8	19.36	0.99	1343.3	22.6	3.28	0.62	A	e	
403.47614.3183	17 55 05.97	-29 20 32.2	20.09	1.14	1323.1	14.4	1.78	2.06	C	e	cv
403.47793.3138 <sup>ad</sup>	17 55 58.04	-29 26 11.6	19.24	1.27	1689.5	19.4	3.01	0.68	B	e	

Note. — After superscripts denote the same event found in multiple objects, events in this table are due to blending of flux from a real event and should be ignored for any analysis. The grades (column 10) are on an A-F scale, and the selection methods (column 11) are “c” for our clump-like selection criteria, “e” for events found by eye, “a” for events found via the alert system, and “b” for events from the binary paper.

Table 5. Alternative designations of our events

field.tile.seq	OGLE	field.tile.seq	OGLE ID
104.20515.498	BUL_SC35_144974	118.19182.891	BUL_SC38_95103
104.20640.8423	BUL_SC35_451130	118.19184.1814	sc38_3314
104.20779.9616	BUL_SC35_770398	118.19184.939	BUL_SC38_120518
104.20906.3973	sc36_6759	119.19442.370	BUL_SC38_627315
105.21287.3893	sc36_1245	119.19701.1513	sc1_1943
108.19073.2291	BUL_SC21_833776	119.19832.5483	BUL_SC1_460673
108.19204.267	BUL_SC30_165305	119.20092.3109	sc45_1286
108.19333.1878	BUL_SC30_352272	119.20219.2348	sc45_810
108.19464.254	BUL_SC30_559419	178.23136.5133	BUL_SC16_436041
108.19464.5201	BUL_SC30_553231	178.23398.4814	BUL_SC17_270411
108.19853.8058	BUL_SC31_513194	308.38595.1020	BUL_SC10_454300
109.19853.2074	BUL_SC31_513194	401.48406.2341	sc20_5229
109.19853.4889	sc31_2369	401.48408.649	BUL_SC20_395103
109.19987.2565	sc32_4302	401.48467.4621	BUL_SC20_391296
109.20370.5166	sc2_3095	402.48158.1296	BUL_SC34_144644
109.20640.360	BUL_SC35_451130	402.48219.2582	sc34_4536
109.20893.3423	BUL_SC33_164492	402.48279.1043	BUL_SC34_639703
113.18674.756	sc21_1395	403.47427.353	sc4_3503
113.18810.2999	BUL_SC21_388360	403.47491.770	BUL_SC4_522952
113.19196.3672	sc30_1782	403.47546.2003	BUL_SC4_463924
113.19325.2001	BUL_SC30_236837	403.47550.807	BUL_SC4_708424
114.19587.3861	BUL_SC31_24931	403.47554.630	BUL_SC4_568740
114.19589.4149	BUL_SC31_48308	403.47669.1859	BUL_SC39_323517
114.20370.6070	sc2_3095	403.47671.57	BUL_SC39_361372
114.20494.3907	BUL_SC2_27414	403.47728.5938	sc39_3550



Table 6. Candidate Sagittarius Events

Event ID	l	b	<i>V</i>	( <i>V</i> − <i>R</i> )
130.28701.2042	4.8512	−6.7517	20.70	0.53
130.28964.2444	5.0507	−6.8103	20.26	0.56
131.29214.519/137.29214.59	4.5149	−7.2331	18.21	0.57
132.30916.803	5.6640	−7.6825	19.14	0.60
132.31306.841	5.7772	−7.8612	19.16	0.63
134.33390.299	6.4858	−8.7196	18.25	0.56
136.27650.2370/142.27650.6057	3.9432	−6.6806	19.90	0.71
137.29210.2447	4.3518	−7.3602	20.16	0.66
137.29731.2320	4.4779	−7.5769	20.19	0.67
137.29986.2769	4.2386	−7.8740	20.56	0.58
139.32203.2073	5.1877	−8.6533	20.27	0.57
142.27776.3952	3.7321	−6.7952	20.91	0.73
144.32453.1528	4.6748	−9.0594	20.43	0.73
148.26586.2310	2.2356	−6.9174	19.72	0.59
148.26590.3689	2.5305	−6.8008	21.24	1.18
149.27233.2244	2.2123	−7.2793	20.71	0.62
149.27237.3033	2.4953	−7.1386	20.87	0.72
150.28409.2370	2.8904	−7.6381	20.48	0.38
151.31133.1607	3.1521	−9.0148	19.88	0.46
152.26320.2643	1.8618	−6.9798	20.17	0.46
152.26964.3183	1.6179	−7.4432	20.41	0.64
153.27488.3450	2.0007	−7.5704	20.55	0.38
153.28787.720/154.28787.2812	2.2335	−8.1667	18.03	0.63
154.29041.2113	1.9448	−8.4379	20.31	0.53
154.29175.2554	2.2214	−8.4213	20.85	0.61
155.26043.1938	0.7719	−7.4219	19.67	0.44
156.27606.899	1.3232	−7.9849	19.12	0.50
166.30682.3768	7.1637	−6.7227	21.19	0.82
172.31579.2624	6.6359	−7.5785	20.37	0.69
172.32358.313	6.7620	−7.9545	18.15	0.58
173.33002.479	6.5333	−8.4153	19.54	0.50
173.33142.1986	7.1540	−8.1955	20.40	0.62
174.29360.352	5.5261	−6.7824	17.59	0.66
175.31446.1290	6.3557	−7.5785	20.96	0.82

Table 6—Continued

Event ID	l	b	V	(V – R)

## REFERENCES

- Alcock, C., et al. 1993, *Nature*, 365, 621  
Alcock, C., et al. 1996, *ApJ*, 463, L67  
Alcock, C., et al. 1997, *ApJ*, 479, 119  
Alcock, C., et al. 1999, *PASP*, 111, 1539  
Alcock, C., et al. 2000a, *ApJ*, 541, 270  
Alcock, C., et al. 2000b, *ApJ*, 541, 734  
Alcock, C., et al. 2000c, *ApJ*, 542, 281  
Alcock, C., et al. 2001, *Nature*, 414, 617  
Afonso, C., et al. 2003, *A&A*, 404, 145  
Aubourg, E. et al. 1993, *Nature*, 265, 623  
Bellazzini, M., Ferraro, F.R., & Buonanno, R. 1999, *MNRAS*, 307, 619  
Bennett, D., et al. 2002, *ApJ*, 579, 639  
Binney, J., Bissantz, N., & Gerhard, O. 2000, *ApJ*, 537, L99  
Bissantz, N., Englmaier, P., Binney, J., & Gerhard, O. 1997, *MNRAS*, 289, 651  
Cavallo, R.M., Cook, K.H., Minniti, D., & Vandehei, T. 2002, preprint (astro-ph/0209196)  
Cseresnjes, P., & Alard, C. 2001, *A&A*, 369, 778  
Evans, N.W. & Belokurov, V. 2002, *ApJ*, 567, L119  
Gaudi, B.S., et al. 2002, *ApJ*, 566, 463  
Girardi, L., Bertelli, G., Bressan, A., Chiosi, C., Groenewegen, M. A. T., Marigo, P., Salasnich, B., Weiss, A. 2002, *A&A*, 391, 195  
Gould, A. & Loeb, A. 1992, *ApJ*, 396, 104  
Gould, A. 2000, *ApJ*, 535, 928  
Griest, K. 1991a, *ApJ*, 366, 412  
Griest, K. et al. 1991b, *ApJ*, 372, L79  
Griest, K. & Safizadeh, N. 1998, *ApJ*, 500, 37  
Gyuk, G. 1999, *ApJ*, 510, 205  
Han, C., & Gould, A., 2003, *ApJ*, 592, 172  
Hart, J., et al. 1996, *PASP*, 108, 220

- Ibata, R.A., Gilmore, G., & Irwin, M.J. 1995, MNRAS, 277, 781  
Kane, S.R., & Sahu, K.C. 2003, ApJ, 582, 743  
Kiraga, M., & Paczyński, B. 1994, ApJ, 430, L101  
Marshall, S.L., et al. 1994, in IAU Symp. 161, Astronomy From Wide Field Imaging, ed. H.T. MacGillivray et al., (Dordrecht: Kluwer)  
Mao, S. & Paczyński, B. 1991, ApJ, 374, L37  
Metcalf, R.B. 1995 ApJ, 110, 869  
Monaco, L., Ferraro, F.R., Ballazzini, M., & Pancino, E. 2002, ApJ, 578, L47  
Nair, V. & Miralda-Escudé, J. 1999, ApJ, 515, 206  
Nemiroff, R.J. 1991, A&A, 247, 73  
Paczyński, B. 1986, ApJ, 304, 1  
Paczyński, B. 1991, ApJ, 371, L63  
Popowski, P., et al. 2001a, ASP Conference Series: ‘Microlensing 2000: A New Era of Microlensing Astrophysics’, eds. J.W. Menzies & P.D. Sackett, Vol. 239, p. 244 (astro-ph/0005466)  
Popowski, P., Cook, K.H., & Becker, A.C. 2003, AJ, 126, 2910  
Popowski, P., et al. 2004 (companion Paper)  
Rhie, S. et al. 2000, ApJ, 533, 378  
Schechter, P.L., Mateo, M. & Saha A. 1993, PASP, 105, 1342  
Sevenster, M.N. & Kalnajs, A.J. 2001, AJ, 122, 885  
Sterken, C., & Jaschek, C., 1996 “Light Curves of Variable Stars”, Cambridge University Press, Cambridge, UK  
Stubbs, C.W., et al. 1993, in Proceedings of the SPIE, Charge Coupled Devices and Solid State Optical Sensors III, ed. M. Blouke, 1900, 192  
Sumi, T., et al. 2003, ApJ, 591, 204  
Udalski, A., et al. 1993, Acta Astron., 43, 69  
Udalski, A., et al. 1994a, ApJ, 426, L69  
Udalski, A., et al. 1994b, Acta Astron., 44, 165  
Udalski, A., et al. 2000, Acta Astron., 50, 307  
Woźniak, P.R., Udalski, A., Szymański, M., Kubiak, M., Pietrzyński, G., Soszyński, I., & Źebruń, K. 2001, Acta Astron., 51, 175

Zhao, H., Spergel, D.N., & Rich, R.M., 1995, ApJ, 440, L13

Zhao, H., & Mao, S. 1996, MNRAS, 283, 1197

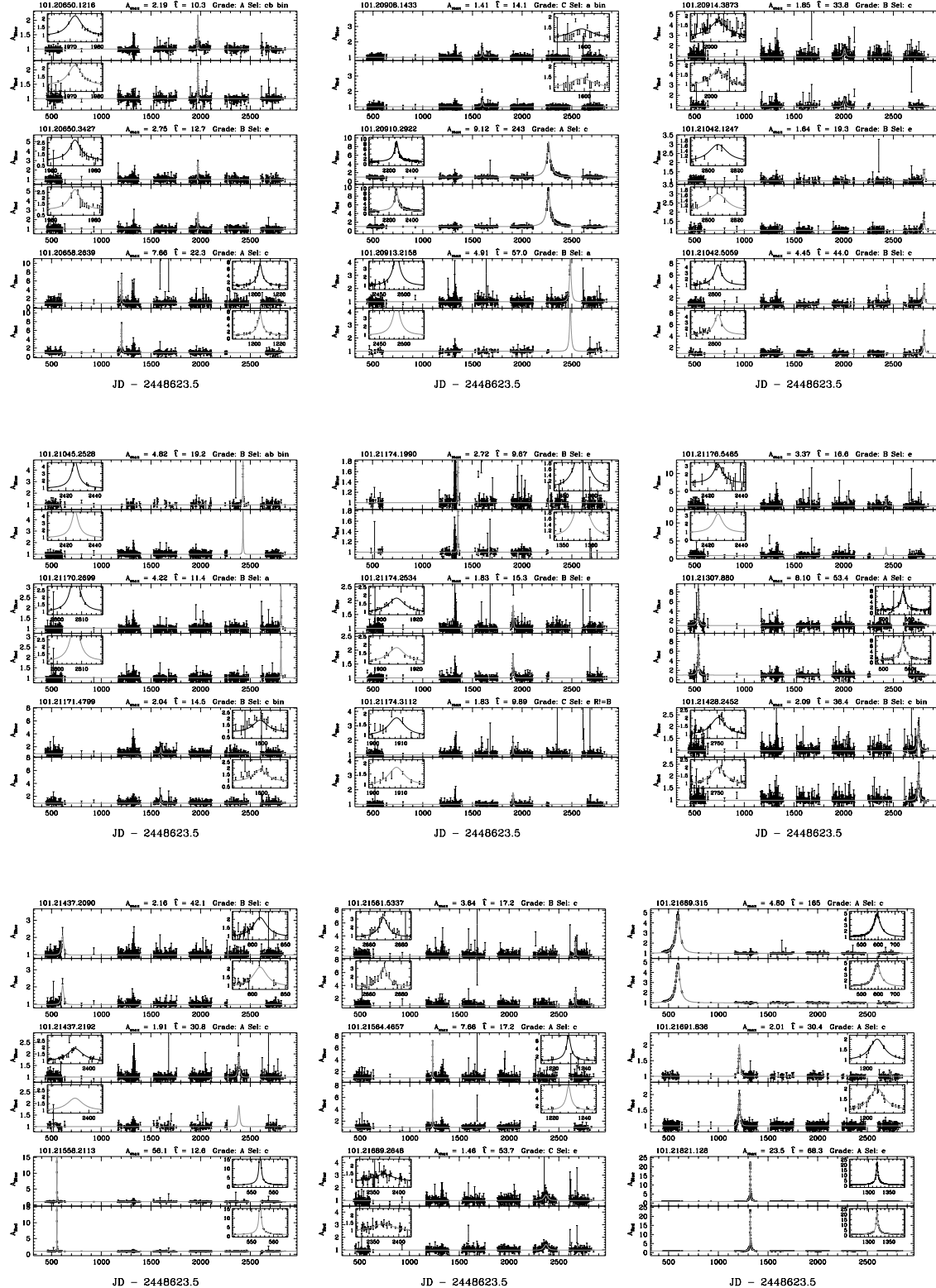


Fig. 10.— Lightcurves of microlensing candidates and some non-microlensing candidates, organized by field.tile.sequence. Also given are  $A_{max}$ ,  $\hat{t}$ , our subjective grade of data quality (A-F), the method by which the event was selected, and any notes concerning our classification of the event.